DOI:10.1158/0008-5472.CAN-10-2438

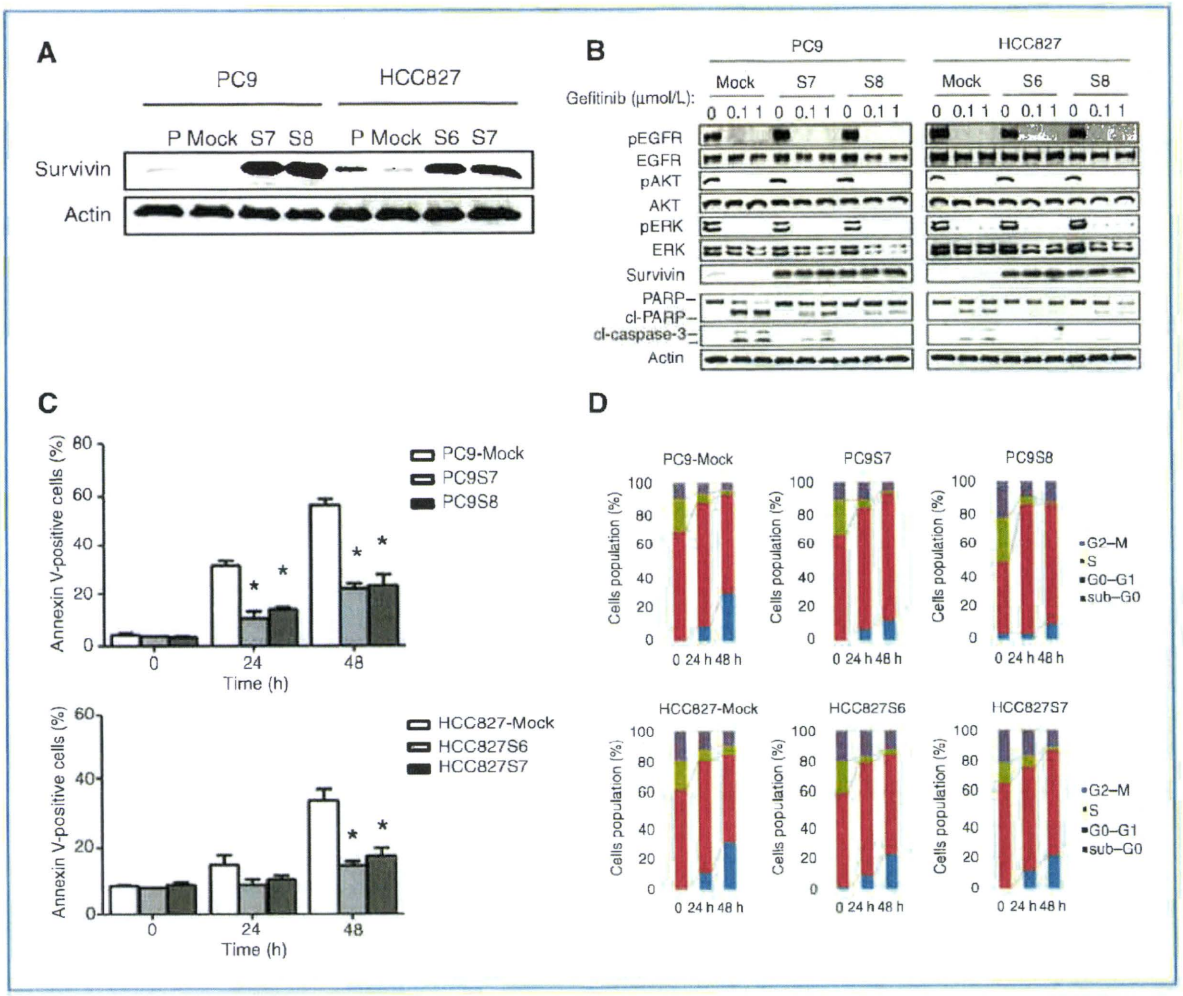

Figure 4. Effect of survivin overexpression on gefitinib-induced apoptosis in *EGFR* mutation–positive NSCLC cells *in vitro*. A, parental (P) PC9 or HCC827 cells or corresponding sublines either stably overexpressing survivin (PC9S7, PC9S8, HCC827S6, and HCC827S7) or infected with the empty retrovirus (PC9-Mock and HCC827-Mock) were cultured overnight in complete medium, after which cell lysates were prepared and subjected to immunoblot analysis with antibodies to survivin or to β-actin. B, PC9 or HCC827 isogenic cell lines were incubated in the presence of the indicated concentrations of gefitinib for 48 hours, after which cell lysates were prepared and subjected to immunoblot analysis with antibodies to phosphorylated (p) or total forms of EGFR, AKT, or ERK, to survivin, to PARP, to caspase-3, or to β-actin. Data in A and B are representative of 3 independent experiments. C, PC9 or HCC827 isogenic cell lines were incubated with gefitinib (0.1 μmol/L) for the indicated times, after which the proportion of apoptotic cells was determined by staining with Annexin V and propidium iodide followed by flow cytometry. Data are means ± SE from 3 independent experiments. *, $P < 0.05$ versus the corresponding value for cells infected with the empty retrovirus. D, PC9 or HCC827 isogenic cell lines were incubated with gefitinib (0.1 μmol/L) for the indicated times and then analyzed for cell cycle distribution by flow cytometry. Data are means of triplicates from representative experiments that were repeated 3 times.

(28, 29). Given that downregulation of survivin through inhibition of the PI3K-AKT pathway was induced by EGFR-TKIs in *EGFR* mutation–positive NSCLC cells and by HER2-targeting agents in breast cancer cells positive for *HER2* amplification, the expression of survivin is likely dependent on PI3K-AKT signaling that operates downstream of receptor tyrosine kinases and is essential for cell survival. This hypothesis is further supported by the observation that transfection of *EGFR* mutation–positive NSCLC cells with an siRNA specific for EGFR mRNA resulted in marked inhibition of survivin expression, whereas transfection of cells expressing wild-type EGFR had no such effect (Supplementary Fig. 2). The PI3K-AKT pathway has been implicated in the regulation of survivin expression by cytokines, growth factors, and chemotherapeutic drugs (8, 10, 30). Although no direct correlation has been established between downregulation of survivin and inhibition of EGFR signaling, these previous findings support the notion that inhibition of the EGFR-PI3K-AKT pathway

DOI:10.1158/0008-5472.CAN-10-2438

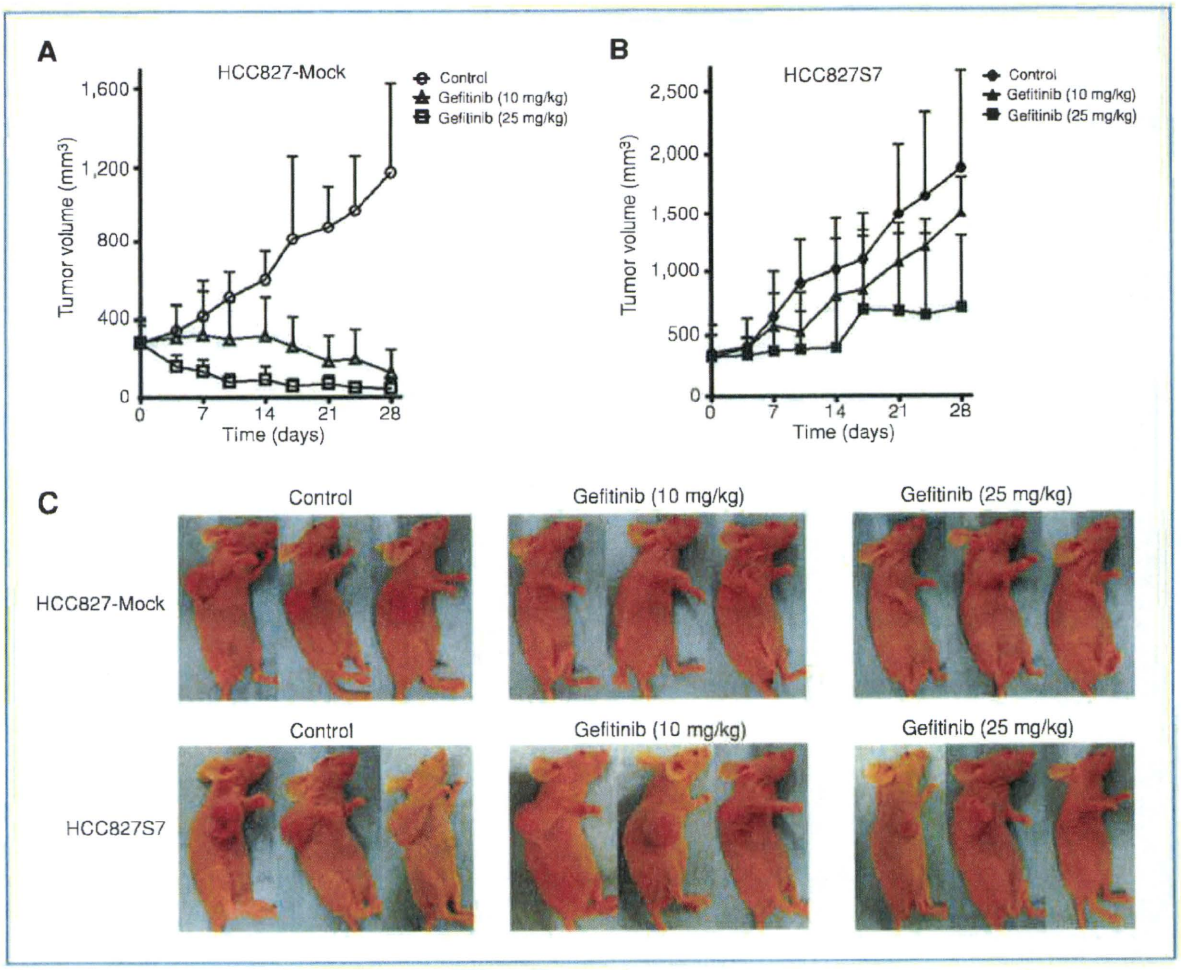

Figure 5. Effect of gefitinib on the growth of *EGFR* mutation–positive NSCLC cells overexpressing survivin *in vivo*. A and B, nude mice with tumor xenografts established by subcutaneous injection of HCC827-Mock or HCC827S7 cells, respectively, were treated daily for 4 weeks with vehicle (control) or gefitinib (10 or 25 mg/kg). Tumor volume was determined at the indicated times after the onset of treatment. Data are means ± SE of values from 6 mice per group. C, representative mice showing tumors at the end of the 4-week treatment period.

contributes to downregulation of survivin expression by EGFR-TKIs in *EGFR* mutation–positive NSCLC cells.

Survivin has been implicated in resistance of cancer cells to apoptosis, although the effect of survivin expression on gefitinib-induced apoptosis in *EGFR* mutation–positive NSCLC cells has not previously been examined. We have now shown that survivin overexpression inhibited gefitinib-induced apoptosis in such cells. Inhibition of the PI3K-AKT and MEK-ERK pathways was previously found to account for much of the proapoptotic activity of EGFR-TKIs in *EGFR* mutation–positive NSCLC cells (31). We further found that overexpression of survivin resulted in inhibition of apoptosis induced by a combination of PI3K and MEK inhibitors in such cells (Supplementary Fig. 3). Increased AKT activity as a result either of the loss of PTEN or of expression of a constitutively active form of AKT was previously found to be associated with a reduced sensitivity to EGFR-TKIs in *EGFR* mutation–positive NSCLC cells (32). However, the principal molecular target underlying the response to inhibition of PI3K-AKT signaling by EGFR-TKIs has remained to be elucidated. In the present study, we show that the sensitivity of *EGFR* mutation–positive NSCLC cells to EGFR-TKIs depends, at least in part, on survivin downregulation through inhibition of the PI3K-AKT pathway. In our xenograft model, we showed that survivin overexpression inhibited the antitumor effect of gefitinib on *EGFR* mutation–positive NSCLC cells. The extent of the clinical benefit of EGFR-TKIs varies among NSCLC patients harboring activating *EGFR* mutations, and the efficacy of these drugs is limited by either *de novo* resistance or resistance acquired after the onset of therapy (33). Although several

DOI:10.1158/0008-5472.CAN-10-2438

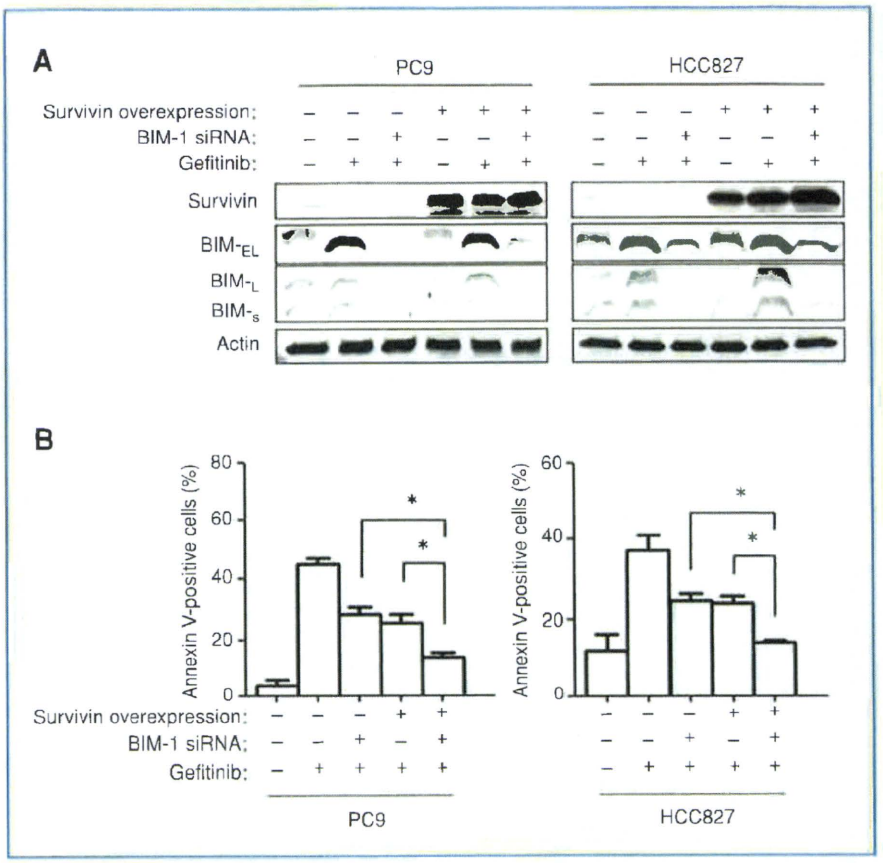

Figure 6. Effect of the combination of survivin overexpression and inhibition of BIM induction on gefitinib-induced apoptosis in *EGFR* mutation–positive NSCLC cells. A, cells stably overexpressing survivin (PC9S7 and HCC827S6) or infected with the empty retrovirus (PC9-Mock and HCC827-Mock) were transfected with BIM (BIM-1) or scrambled siRNAs for 24 hours and then incubated for 24 hours in complete medium with or without gefitinib (0.1 μmol/L). Cell lysates were then prepared and subjected to immunoblot analysis with antibodies to survivin, to BIM, or to β-actin. Data are representative of 3 independent experiments. B, cells transfected as in (A) were incubated for 48 hours in the absence or presence of gefitinib (0.1 μmol/L) and then evaluated for the proportion of apoptotic cells by staining with Annexin V and propidium iodide followed by flow cytometry. Data are means ± SE from 3 independent experiments. *, $P < 0.05$ for the indicated comparisons.

mechanisms of acquired resistance have been described, it remains of clinical concern that molecular markers for prediction of *de novo* resistance to these drugs have not been well delineated (23, 34–38). It will therefore be of interest to determine whether increased survivin expression in tumors is clinically useful as a negative predictive marker of sensitivity to EGFR-TKIs in patients with *EGFR* mutation–positive NSCLC.

Our observations revealed that survivin overexpression did not completely abolish gefitinib-induced apoptosis, suggesting that another proapoptotic regulator activated after EGFR inhibition might contribute to EGFR-TKI–induced apoptotic cell death. Previous studies have shown that gefitinib induces BIM expression via inhibition of the MEK-ERK pathway and that BIM induction plays a key role in EGFR-TKI–induced apoptosis in *EGFR* mutation–positive NSCLC cells (25–27). We have now shown that inhibition of both survivin downregulation and BIM induction attenuated gefitinib-induced apoptosis to a greater extent than did inhibition of either process alone. The recent preclinical study showing that the combination of a PI3K inhibitor and a MEK inhibitor, but neither agent alone, induced substantial growth inhibition in *EGFR* mutation–positive NSCLC cells (31) supports the notion that both the PI3K-AKT-survivin and MEK-ERK-BIM pathways contribute independently to gefitinib-induced apoptosis in such cells (Fig. 7).

In conclusion, we have shown that the EGFR-TKI gefitinib downregulated survivin expression, likely through inhibition

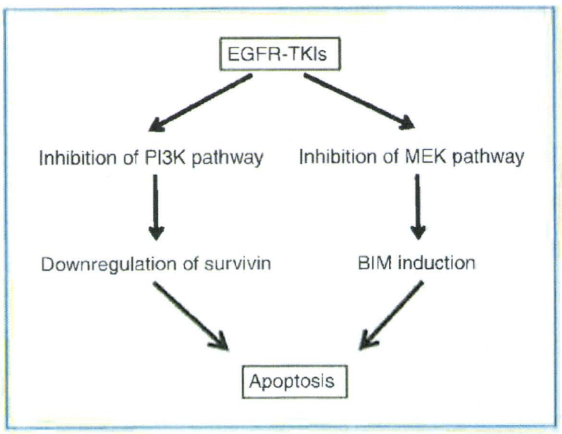

Figure 7. Proposed model for the intracellular signaling underlying EGFR-TKI–induced apoptosis in *EGFR* mutation–positive NSCLC cells.

DOI:10.1158/0008-5472.CAN-10-2438

of PI3K-AKT signaling, and that this effect plays a key role in gefitinib-induced apoptosis. Moreover, we found that survivin downregulation and BIM induction are independently required for EGFR-TKI–induced apoptosis. Our results thus show that simultaneous upstream interruption of the PI3K-AKT-survivin and MEK-ERK-BIM pathways mediates EGFR-TKI–induced apoptosis.

References

1. Blanc-Brude OP, Mesri M, Wall NR, Plescia J, Dohi T, Altieri DC. Therapeutic targeting of the survivin pathway in cancer: initiation of mitochondrial apoptosis and suppression of tumor-associated angiogenesis. Clin Cancer Res 2003;9:2683–92.
2. Dohi T, Okada K, Xia F, et al. An IAP-IAP complex inhibits apoptosis. J Biol Chem 2004;279:34087–90.
3. Li F, Ambrosini G, Chu EY, et al. Control of apoptosis and mitotic spindle checkpoint by survivin. Nature 1998;396:580–4.
4. Ambrosini G, Adida C, Altieri DC. A novel anti-apoptosis gene, survivin, expressed in cancer and lymphoma. Nat Med 1997;3:917–21.
5. Ambrosini G, Adida C, Sirugo G, Altieri DC. Induction of apoptosis and inhibition of cell proliferation by survivin gene targeting. J Biol Chem 1998;273:11177–82.
6. Kallio MJ, Nieminen M, Eriksson JE. Human inhibitor of apoptosis protein (IAP) survivin participates in regulation of chromosome segregation and mitotic exit. FASEB J 2001;15:2721–3.
7. Li F, Altieri DC. The cancer antiapoptosis mouse survivin gene: characterization of locus and transcriptional requirements of basal and cell cycle-dependent expression. Cancer Res 1999;59:3143–51.
8. Carter BZ, Milella M, Altieri DC, Andreeff M. Cytokine-regulated expression of survivin in myeloid leukemia. Blood 2001;97:2784–90.
9. Fang ZH, Dong CL, Chen Z, et al. Transcriptional regulation of survivin by c-Myc in BCR/ABL-transformed cells: implications in anti-leukaemic strategy. J Cell Mol Med 2009;13:2039–52.
10. Beierle EA, Nagaram A, Dai W, Iyengar M, Chen MK. VEGF-mediated survivin expression in neuroblastoma cells. J Surg Res 2005;127:21–8.
11. Tran J, Master Z, Yu JL, Rak J, Dumont DJ, Kerbel RS. A role for survivin in chemoresistance of endothelial cells mediated by VEGF. Proc Natl Acad Sci U S A 2002;99:4349–54.
12. Fan J, Wang L, Jiang GN, He WX, Ding JA. The role of survivin on overall survival of non-small cell lung cancer, a meta-analysis of published literatures. Lung Cancer 2008;61:91–6.
13. Huang CL, Liu D, Nakano J, et al. E2F1 overexpression correlates with thymidylate synthase and survivin gene expressions and tumor proliferation in non small-cell lung cancer. Clin Cancer Res 2007;13:6938–46.
14. Krepela E, Dankova P, Moravcikova E, et al. Increased expression of inhibitor of apoptosis proteins, survivin and XIAP, in non-small cell lung carcinoma. Int J Oncol 2009;35:1449–62.
15. Mendelsohn J, Baselga J. The EGF receptor family as targets for cancer therapy. Oncogene 2000;19:6550–65.
16. Schlessinger J. Cell signaling by receptor tyrosine kinases. Cell 2000;103:211–25.
17. Hynes NE, Lane HA. ERBB receptors and cancer: the complexity of targeted inhibitors. Nat Rev Cancer 2005;5:341–54.
18. Paez JG, Janne PA, Lee JC, et al. EGFR mutations in lung cancer: correlation with clinical response to gefitinib therapy. Science 2004;304:1497–500.
19. Shepherd FA, Rodrigues Pereira J, Ciuleanu T, et al. Erlotinib in previously treated non-small-cell lung cancer. N Engl J Med 2005;353:123–32.
20. Sordella R, Bell DW, Haber DA, Settleman J. Gefitinib-sensitizing EGFR mutations in lung cancer activate anti-apoptotic pathways. Science 2004;305:1163–7.
21. Tracy S, Mukohara T, Hansen M, Meyerson M, Johnson BE, Janne PA. Gefitinib induces apoptosis in the EGFRL858R non-small-cell lung cancer cell line H3255. Cancer Res 2004;64:7241–4.
22. Ling YH, Lin R, Perez-Soler R. Erlotinib induces mitochondrial-mediated apoptosis in human H3255 non-small-cell lung cancer cells with epidermal growth factor receptorL858R mutation through mitochondrial oxidative phosphorylation-dependent activation of BAX and BAK. Mol Pharmacol 2008;74:793–806.
23. Koizumi F, Shimoyama T, Taguchi F, Saijo N, Nishio K. Establishment of a human non-small cell lung cancer cell line resistant to gefitinib. Int J Cancer 2005;116:36–44.
24. Tanaka K, Arao T, Maegawa M, et al. SRPX2 is overexpressed in gastric cancer and promotes cellular migration and adhesion. Int J Cancer 2009;124:1072–80.
25. Costa DB, Halmos B, Kumar A, et al. BIM mediates EGFR tyrosine kinase inhibitor-induced apoptosis in lung cancers with oncogenic EGFR mutations. PLoS Med 2007;4:1669–79; discussion 80.
26. Cragg MS, Kuroda J, Puthalakath H, Huang DC, Strasser A. Gefitinib-induced killing of NSCLC cell lines expressing mutant EGFR requires BIM and can be enhanced by BH3 mimetics. PLoS Med 2007;4:1681–89; discussion 90.
27. Gong Y, Somwar R, Politi K, et al. Induction of BIM is essential for apoptosis triggered by EGFR kinase inhibitors in mutant EGFR-dependent lung adenocarcinomas. PLoS Med 2007;4:1655–68.
28. Asanuma H, Torigoe T, Kamiguchi K, et al. Survivin expression is regulated by coexpression of human epidermal growth factor receptor 2 and epidermal growth factor receptor via phosphatidylinositol 3-kinase/AKT signaling pathway in breast cancer cells. Cancer Res 2005;65:11018–25.
29. Xia W, Bisi J, Strum J, et al. Regulation of survivin by ErbB2 signaling: therapeutic implications for ErbB2-overexpressing breast cancers. Cancer Res 2006;66:1640–7.
30. Zhao P, Meng Q, Liu LZ, You YP, Liu N, Jiang BH. Regulation of survivin by PI3K/Akt/p70S6K1 pathway. Biochem Biophys Res Commun 2010;395:219–24.
31. Faber AC, Li D, Song Y, et al. Differential induction of apoptosis in HER2 and EGFR addicted cancers following PI3K inhibition. Proc Natl Acad Sci U S A 2009;106:19503–8.
32. Sos ML, Koker M, Weir BA, et al. PTEN loss contributes to erlotinib resistance in EGFR-mutant lung cancer by activation of Akt and EGFR. Cancer Res 2009;69:3256–61.
33. Okamoto I. Epidermal growth factor receptor in relation to tumor development: EGFR-targeted anticancer therapy. FEBS J 2009;277:309–15.
34. Engelman JA, Zejnullahu K, Mitsudomi T, et al. MET amplification leads to gefitinib resistance in lung cancer by activating ERBB3 signaling. Science 2007;316:1039–43.
35. Ercan D, Zejnullahu K, Yonesaka K, et al. Amplification of EGFR T790M causes resistance to an irreversible EGFR inhibitor. Oncogene 2010;29:2346–56.
36. Pao W, Miller VA, Politi KA, et al. Acquired resistance of lung adenocarcinomas to gefitinib or erlotinib is associated with a second mutation in the EGFR kinase domain. PLoS Med 2005;2:225–35.
37. Yano S, Wang W, Li Q, et al. Hepatocyte growth factor induces gefitinib resistance of lung adenocarcinoma with epidermal growth factor receptor-activating mutations. Cancer Res 2008;68:9479–87.
38. Takeda M, Okamoto I, Fujita Y, et al. *De novo* resistance to epidermal growth factor receptor-tyrosine kinase inhibitors in EGFR mutation-positive patients with non-small cell lung cancer. J Thorac Oncol 2010;5:399–400.

Disclosure of Potential Conflicts of Interest

No potential conflicts or interest were disclosed.

The costs of publication of this article were defrayed in part by the payment of page charges. This article must therefore be hereby marked *advertisement* in accordance with 18 U.S.C. Section 1734 solely to indicate this fact.

Received 07/06/2010; revised 09/11/2010; accepted 10/08/2010; published Online 12/15/2010.

Cancer Science
The official journal of the Japanese Cancer Association JCA

Plasma concentrations of VCAM-1 and PAI-1: A predictive biomarker for post-operative recurrence in colorectal cancer

Yasuhide Yamada,[1,8] Tokuzo Arao,[2,8] Kazuko Matsumoto,[2] Vinita Gupta,[3] Woei Tan,[3] Joe Fedynyshyn,[3] Takako E. Nakajima,[1] Yasuhiro Shimada,[1] Tetsuya Hamaguchi,[1] Ken Kato,[1] Hirokazu Taniguchi,[4] Yutaka Saito,[5] Takahisa Matsuda,[5] Yoshihiro Moriya,[6] Takayuki Akasu,[6] Shin Fujita,[6] Seiichiro Yamamoto[6] and Kazuto Nishio[2,7]

[1]Medical Oncology, National Cancer Center Hospital, Tokyo, Japan; [2]Department of Genome Biology, Kinki University School of Medicine, Osaka, Japan; [3]Bio-Rad Laboratories, Hercules, California, USA; [4]Diagnostic Pathology Division, [5]Endoscopic Division, [6]Surgical Division, National Cancer Center Hospital, Tokyo, Japan

(Received December 2, 2009/Revised March 29, 2010/Accepted April 9, 2010/Accepted manuscript online April 21, 2010)

This prospective study used antibody suspension bead arrays to identify biomarkers capable of predicting post-operative recurrence with distal metastasis in patients with colorectal cancer. One hundred colorectal cancer patients who underwent surgery were enrolled in this study. The median follow-up period was 3.9 years. The pre-operative plasma concentrations of 24 angiogenesis-related molecules were analyzed with regard to the TNM stage and the development of post-operative recurrence. The concentrations of half of the examined molecules (13/24) increased significantly according to the TNM stage ($P < 0.05$). Meanwhile, a multivariate logistic regression analysis revealed that the concentrations of vascular cell adhesion molecule 1 (VCAM-1) and plasminogen activator inhibitor-1 (PAI-1) were significantly higher in the post-operative recurrence group. The VCAM-1 and PAI-1 model discriminated post-operative recurrence with an area under the curve of 0.82, a sensitivity of 0.75, and a specificity of 0.73. A leave-one-out cross-validation was applied to the model to assess the prediction performance, and the result indicated that the cross-validated error rate was 12.5% (12/96). In conclusion, our results demonstrate that antibody suspension bead arrays are a powerful tool to screen biomarkers in the clinical setting, and the plasma levels of VCAM-1 and PAI-1 together may be a promising biomarker for predicting post-operative recurrence in patients with colorectal cancer. (*Cancer Sci* 2010)

Colorectal cancer (CRC) is one of the leading causes of death in Japan (http://ganjoho.ncc.go.jp/public/statistics/index.html) and Western countries.[1] Despite recent advances in adjuvant chemotherapy and surgical techniques, 20–40% of patients die because of metastasis after curative surgery.[2] Tumor-node-metastasis (TNM) staging is well established and the most reliable system for predicting the outcome of CRC. In particular, the TNM staging system works very well for predicting the outcome of early stage I cancers and advanced stage IV cancers. However, the 5-year survival rate varies from 44% to 83% within TNM stage III, indicating that a wide variation in outcomes exists within each stage as a result of biological heterogeneity.[3] Thus, highly accurate predictors of post-operative recurrence are needed for patients with CRC who undergo curative surgery, as such predictors would likely contribute to the further improvement of the 5-year survival rate by justifying the addition of intensive adjuvant chemotherapy to the therapeutic regimens of subgroups with a high risk of post-operative recurrence. Therefore, the prediction of post-operative recurrence is regarded as one of the most important research themes in clinical settings and has been extensively studied, with particular attention given to the investigation of various molecular prognostic factors.

In addition to the TNM stage, the carcinoembryonic antigen (CEA) level is routinely used to monitor recurrence in patients with CRC.[4] A large clinical study demonstrated that pre-operative CEA levels provide prognostic information in addition to that provided by the TNM staging system and determined that the pre-operative CEA level was an independent predictor of survival and recurrence.[5] However, the study concluded that although an elevated pre-operative CEA level (>5 mg/mL) may be correlated with a poor prognosis, the available data was insufficient to support the use of the CEA level for determining whether a patient should undergo adjuvant therapy.[4] Other molecular markers, including the K-Ras mutation status,[6,7] microsatellite instability,[8] the loss of heterogeneity at 18q,[9] and p53,[10] have been examined with regard to predicting the outcome of subgroups; unfortunately, none of these molecular markers are suitable for routine clinical use. Thus, further investigations of novel molecular markers are eagerly awaited.

The Bio-Plex suspension array system (Bio-Rad Laboratories, Hercules, CA, USA) utilizes a series of color-coded beads, each of which is coupled to a unique antibody specific for a biochemical marker. This assay is capable of measuring the levels of multiple targets in a single well of a 96-well microplate using as little as 12.5 μL of serum, plasma, or other matrix. In the present study, 24 angiogenesis-related markers from this assay panel were used to evaluate plasma proteins and their potential associations with disease progression and the recurrence of CRC.

Materials and Methods

Patient selection. Patients with histologically confirmed colorectal cancer who were between the ages of 20 and 80 years and who were scheduled to undergo surgery were eligible for enrollment in this study. Additional inclusion criteria included an Eastern Cooperative Oncology Group performance status of 0–2. All the patients in this series underwent surgery. This prospective study was approved by the Institutional Review Board of the National Cancer Center Hospital and written informed consent was obtained from all the patients.

Clinical and pathologic features. Clinical features including age, sex, primary site of tumor, histologic type of tumor, TNM stage, and post-operative recurrence were recorded. A pathologist reviewed the microscopic slides. Post-operative recurrence was defined when distant metastasis was observed. The median follow-up period of post-operative recurrence was 3.9 years.

[7]To whom correspondence should be addressed.
E-mail: knishio@med.kindai.ac.jp
[8]These authors contributed equally to this work.

doi: 10.1111/j.1349-7006.2010.01595.x

Preparation of plasma samples. Two milliliters of whole blood were collected into EDTA-containing tubes before surgery (within 2 weeks) and were centrifuged at 1500 *g* for 10 min to obtain the plasma samples. The samples were stored at −80°C until further use.

Angiogenesis-related molecules. The 24 plasma markers used in this study were as follows: interleukin 6 receptor (IL-6R), matrix metallopeptidase 9 (MMP-9), TIMP metallopeptidase inhibitor 1 (TIMP-1), TIMP metallopeptidase inhibitor 2 (TIMP-2), endostatin, P-selectin, intercellular adhesion molecule 1 (ICAM-1), vascular cell adhesion molecule 1 (VCAM-1), Tie-2, plasminogen activator inhibitor-1 (PAI-1), macrophage migration inhibitory factor (MIF), plasminogen activator urokinase receptor (uPAR), angiopoietin 2 (Ang-2), follistatin, hepatocyte growth factor (HGF), interleukin 8 (IL-8), colony stimulating factor 3 (G-CSF), platelet-derived growth factor beta polypeptide (PDGF-BB), vascular endothelial growth factor (VEGF), leptin, platelet/endothelial cell adhesion molecule (PECAM-1), interleukin 12 (IL-12), fibroblast growth factor 2 (FGF-basic), and tumor necrosis factor (TNF-α). Ang-2, Follistatin, The nine markers of HGF, IL-8, PDGF-BB, VEGF, Leptin, PECAM-1, and G-CSF are commercially available as the Human Premixed Angiogenesis (9) panel (Bio-Rad Laboratories). The others are available for customization or in developing markers.

Antibody suspension bead arrays system. The plasma concentrations of each molecule were measured using a Bio-Plex suspension array system (Bio-Rad Laboratories), which permits the simultaneous measurement of multiple circulating proteins in a single well using only 12.5 μL of plasma. The assay was performed according to the manufacturer's instructions and a previously described method.[11] All plasma samples were diluted 1 in 4 with the appropriate diluents prior to assay. The samples were tested in duplicate.

Statistical analysis. The correlations between the plasma concentrations and the TNM stages were analyzed using a linear trend analysis and the proportional odds model. In the linear trend analysis, we used a one-way ANOVA model with a linear contrast, which consisted of the TMN stage scores. A *t*-test was used to compare the post-operative recurrence and the no recurrence groups. In the multivariate analysis, an analysis was performed for all the plasma markers but not for the clinical variables because too many explanatory variables for the sample size were included in this study. A logistic regression analysis was used to examine statistical differences according to post-operative recurrence and a stepwise method was used to select the most useful explanatory parameters. Analyses were performed using SAS software version 9.1.3 (SAS Institute, Cary, NC, USA). A *P*-value of <0.05 was considered statistically significant.

Results

Patient results. A total of 100 consecutive patients were enrolled in this study. The median age of the enrolled patients was 59 years (range, 31–79 years). Among them, 96 patients received curative operations and four patients had distal metastasis and received palliative operations. Eleven patients developed recurrences with distal metastasis during the follow-up period. Table 1 summarizes the characteristics of the patients and their tumors.

Plasma concentrations of 24 angiogenesis-related molecules. We measured the plasma concentrations of 24 angiogenesis-related molecules: IL-6R, MMP-9, TIMP-1, TIMP-2, endostatin, P-selectin, ICAM-1, VCAM-1, Tie-2, PAI-1, MIF, uPAR, Ang-2, follistatin, HGF, IL-8, G-CSF, PDGF-BB, VEGF, leptin, PECAM-1, IL-12, FGF-basic, and TNF-α (Table 2). Overall, 98.5% of the plasma samples were successfully quantified using a standard curve.

Table 1. Patient characteristics

Characteristics	Curative ope.		Palliative ope.	Total
	Rec+	Rec−		
Age (years)				
≥60	6	42	2	50
<60	5	43	2	50
Sex				
Male	3	54	3	65
Female	8	31	1	35
Primary site				
Colon	8	40	1	49
Rectum	3	45	3	51
Hist. type				
Well diff.	8	59	3	70
Others	3	26	1	30
TNM stage				
I	1	26	–	27
II	2	22	–	24
III	8	37	–	45
IV	–	–	4	4
Total	11	85	4	100

Hist. type, histology of primary tumor; Rec+, post-operative recurrence (+); Rec−, post-operative recurrence (−).

Tumor-node-metastasis (TNM) stage and plasma concentrations of angiogenesis-related molecules. The TNM stage can be accurately used to stratify patients at a high risk for cancer progression and is thought to reflect the malignant potential of each tumor. To estimate the contributions of the angiogenesis-related molecules to the malignant potentials of the tumors, we examined the correlation between the plasma concentrations of each molecule and the TNM stage. A linear trend analysis showed that the plasma concentrations of 13 molecules increased significantly with an increasing TNM stage ($P < 0.05$): IL-6R, TIMP-1, TIMP-2, P-selectin, Tie-2, PAI-1, uPAR, Ang-2, follistatin, HGF, IL-8, PDGF-BB, and VEGF (Table 3). Next, we performed an exploratory multivariate analysis using a proportional odds model with the TNM stage (I–IV) assigned as the objective variable and each of the angiogenesis-related molecules assigned as explanatory variables. The multivariate analysis identified TIMP-1, P-selectin, Ang-2, HGF, IL-8, PDGF-BB, and VEGF as being significantly correlated with the TNM stage. These results indicated that the plasma concentrations of several molecules increased significantly with an increasing TNM stage, strongly suggesting that these molecules might be candidate biomarkers for an unfavorable outcome in patients with CRC.

Post-operative recurrence and plasma concentrations of angiogenesis-related molecules. To predict post-operative recurrence using this system, we analyzed the 96 patients with CRC who underwent curative operations, excluding the four patients with distal metastasis. Among these 96 patients, 11 developed recurrences during the follow-up period; the remaining 85 patients did not show any signs of recurrence. When the plasma levels of the angiogenesis-related molecules were compared between the patients with recurrences and those without recurrences, *t*-tests demonstrated that the plasma concentrations of IL-6R (63.2 ± 13.8 and 51.3 ± 17.0 ng/mL, respectively), P-selectin (76.1 ± 24.4 and 60.0 ± 24.8 ng/mL, respectively), VCAM-1 (163.9 ± 61.0 and 134.6 ± 35.0 ng/mL, respectively), and PAI-1 (28.2 ± 15.4 and 19.8 ± 10.2 ng/mL, respectively) were significantly higher among the patients with recurrences (Fig. 1a–d, Table 4). A multivariate logistic regression analysis revealed that the plasma concentrations of VCAM-1 and PAI-1 were significantly higher among the patients with recurrences ($P = 0.039$ and $P = 0.028$, respectively). A stepwise

doi: 10.1111/j.1349-7006.2010.01595.x

Table 2. Plasma concentrations of 24 angiogenesis-related molecules in 100 colorectal cancers

Molecules	Range	Average (SD)	25%	Percentile	
	pg/mL			Median	75%
IL-6R	23–149	54 (18)	42	52	62
MMP-9	6–189	35 (27)	20	27	41
TIMP-1	44–283	117 (35)	96	118	135
TIMP-2	9–47	24 (5)	21	24	28
Endostatin	90–456	187 (64)	140	177	223
P-selectin	0–164	64 (27)	48	62	78
ICAM-1	103–605	282 (81)	225	270	317
VCAM-1	76–333	138 (40)	110	135	163
Tie-2	9–1070	143 (164)	48	73	182
PAI-1	3–65	21 (12)	14	19	26
MIF	0–120	53 (26)	44	59	69
uPAR	1–130	24 (23)	8	15	37
Ang-2	0–6147	1381 (1337)	415	938	2197
Follistatin	235–2903	924 (614)	502	686	1197
HGF	201–12213	2700 (2516)	1076	1628	3930
IL-8	5–234	52 (41)	24	34	74
G-CSF	0–4775	832 (1133)	79	247	1161
PDGF-BB	6–6219	737 (831)	220	439	922
VEGF	0–724	186 (164)	67	120	262
Leptin	0–32847	3155 (4433)	1149	2134	3851
PECAM-1	1188–15837	5562 (3472)	2901	4487	7348
IL-12	0–32	5 (6)	2	3	6
FGF-basic	0–235	21 (30)	4	13	25
TNF-α	0–72	4 (9)	1	2	4

The concentrations are ng/mL for interleukin 6 receptor (IL-6R), matrix metallopeptidase 9 (MMP-9), TIMP metallopeptidase inhibitor 1 (TIMP-1), TIMP-2, endostatin, P-selectin, intercellular adhesion molecule 1 (ICAM-1), vascular cell adhesion molecule 1 (VCAM-1), Tie-2, plasminogen activator inhibitor-1 (PAI-1), macrophage migration inhibitory factor (MIF), and plasminogen activator urokinase receptor (uPAR), and the others are pg/mL. FGF-basic, fibroblast growth factor 2; G-CSF, colony stimulating factor 3; HGF, hepatocyte growth factor; PDGF-BB, platelet-derived growth factor beta polypeptide; PECAM-1, platelet/endothelial cell adhesion molecule; TNF-α, tumor necrosis factor; VEGF, vascular endothelial growth factor.

Table 3. Tumor-node-metastasis (TNM) stage and plasma concentrations in 100 colorectal cancers

Molecules	TNM stage				Univariate	Multivariate
	I	II	III	IV	*P*-value	*P*-value
IL-6R	50	57	52	76	0.01	n.s.
MMP-9	34	50	28	33	n.s.	n.s.
TIMP-1	107	122	114	185	<0.0001	0.02
TIMP-2	24	24	24	33	0.003	n.s.
Endostatin	184	198	182	201	n.s.	n.s.
P-selectin	56	67	63	109	0.0003	0.04
ICAM-1	276	315	266	298	n.s.	n.s.
VCAM-1	135	136	141	144	n.s.	n.s.
Tie-2	116	162	129	375	0.005	n.s.
PAI-1	18	24	21	38	0.003	n.s.
MIF	53	55	51	78	n.s.	n.s.
uPAR	20	27	22	53	0.01	n.s.
Ang-2	978	1458	1447	2914	0.007	0.03
Follistatin	778	953	928	1704	0.006	n.s.
HGF	1933	2932	2803	5342	0.01	0.04
IL-8	38	56	53	108	0.002	0.02
G-CSF	595	1114	797	1132	n.s.	n.s.
PDGF-BB	442	822	802	1483	0.02	0.03
VEGF	129	209	192	375	0.006	0.03
Leptin	3236	2815	3235	3752	n.s.	n.s.
PECAM-1	5026	5914	5625	6356	n.s.	n.s.
IL-12	3	8	5	5	n.s.	n.s.
FGF-basic	19	32	16	28	n.s.	n.s.
TNF-α	4	6	3	2	n.s.	n.s.

Values indicate the average. Univariate: linear trend analysis, multivariate: proportional odds model. The concentrations are ng/mL for interleukin 6 receptor (IL-6R), matrix metallopeptidase 9 (MMP-9), TIMP metallopeptidase inhibitor 1 (TIMP-1), TIMP-2, endostatin, P-selectin, intercellular adhesion molecule 1 (ICAM-1), vascular cell adhesion molecule 1 (VCAM-1), Tie-2, plasminogen activator inhibitor-1 (PAI-1), macrophage migration inhibitory factor (MIF), and plasminogen activator urokinase receptor (uPAR), and the others are pg/mL. FGF-basic, fibroblast growth factor 2; G-CSF, colony stimulating factor 3; HGF, hepatocyte growth factor; n.s., not significant; PDGF-BB, platelet-derived growth factor beta polypeptide; PECAM-1, platelet/endothelial cell adhesion molecule; TNF-α, tumor necrosis factor; VEGF, vascular endothelial growth factor.

method selected VCAM-1 and PAI-1 as the most useful explanatory parameters, suggesting that the combination of these two molecules might synergistically improve the prediction of post-operative recurrence. Finally, a prediction model incorporating VCAM-1 and PAI-1 successfully discriminated post-operative recurrence, with an area under the curve (AUC) of 0.82, a sensitivity of 0.75, and a specificity of 0.73 (Fig. 2a). To assess the prediction performance, a leave-one-out cross-validation was applied to the model. The cross-validated error rate was 12.5% (12/96). In stage III patients, the prediction model had a sensitivity of 0.625 (5/8) and a specificity of 0.865 (32/37) for predicting post-operative recurrence (Fig. S2). On the other hand, when apparent distal metastases of CRCs were applied to the VCAM-1/PAI-1 prediction model, three out of four metastatic cases were determined as "recurrence (+) cases". These results suggest that apparent metastatic tumors could be discriminated using the model. Although a validation study is necessary, our results raise the possibility that the combined use of the pre-operative plasma concentrations of VCAM-1 and PAI-1 might be useful for predicting post-operative recurrence in patients with CRC. Finally, we retrospectively analyzed the plasma PAI-1 concentrations of metastatic and non-metastatic CRC in another study of an independent cohort using conventional ELISA. The plasma concentrations in the metastatic CRC patients were significantly higher than those in the non-metastatic patients ($P = 0.005$), even in the independent cohort (Fig. S1). The CEA level was not significantly different between the recurrence (+) *versus* the recurrence (−) groups ($P = 0.335$) in our study.

Discussion

Vascular cell adhesion molecule 1 (VCAM-1)/CD106 is a member of the Ig superfamily and encodes a cell surface sialoglycoprotein expressed by cytokine-activated endothelium. This type I membrane protein mediates leukocyte-endothelial cell adhesion and signal transduction, and may play a role in the development of atherosclerosis[12] and rheumatoid arthritis.[13] In the field of oncology, accumulating evidence suggests that VCAM-1 is associated with a poor outcome.[14–17] Recently, Shariat *et al.*[18] reported that standard clinical variables alone exhibited an accuracy of 71.6% for predicting the risk of biochemical recurrence following a radical prostatectomy in patients with prostate cancer, whereas the addition of preoperative blood levels of TGF-β1, sIL-6R, IL-6, VCAM-1, VEGF, endoglin, and uPA increased the predictive accuracy by 15–86.6%. Vascular endothelial growth factor (VEGF) and uPA were not significant predictors of post-operative recurrence in our data set for CRC, but VCAM-1 and sIL-6R were significant, consistent with Shariat's study. The mechanism by which VCAM-1 mediates an unfavorable phenotype remains unclear, but the most probable explanation is that the tumor cells escape T-cell immunity by

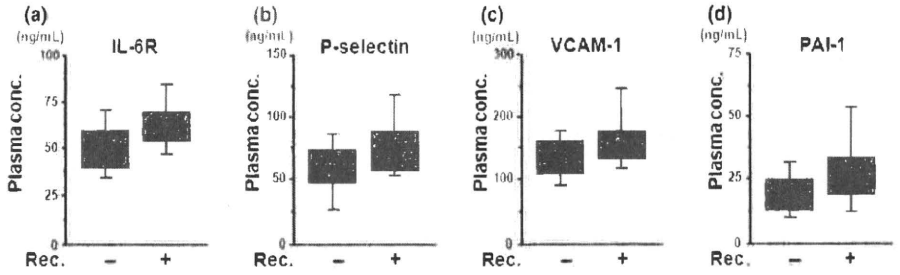

Fig. 1. The concentrations of (a) interleukin 6 receptor (IL-6R), (b) P-selectin, (c) vascular cell adhesion molecule 1 (VCAM-1), and (d) plasminogen activator inhibitor-1 (PAI-1) were significantly higher in the recurrence group in colorectal cancer. The upper bar, box, and lower bar represent the 90%, 75%, 50%, 25% and 10% percentiles. The plasma concentrations of each molecule were measured using a Bio-Plex suspension array system. Rec, recurrence.

Table 4. Results of multivariate analysis for recurrence after curative surgery in 96 colorectal cancers

Molecules	Recurrence*		Univariate		Multivariate
	+	–	*t*-test	Logistic	Stepwise
			P-value	*P*-value	*P*-value
IL-6R	63	51	0.03	n.s.	
MMP-9	37	35	n.s.	n.s.	
TIMP-1	119	113	n.s.	n.s.	
TIMP-2	25	24	n.s.	n.s.	
Endostatin	193	186	n.s.	n.s.	
P-selectin	76	60	0.04	n.s.	
ICAM-1	285	281	n.s.	n.s.	
VCAM-1	164	135	0.02	0.039	0.009
Tie-2	183	127	n.s.	n.s.	
PAI-1	28.3	19.8	0.02	0.005	0.005
MIF	64	51	n.s.	n.s.	
uPAR	30	21	n.s.	n.s.	
Ang-2	1514	1292	n.s.	n.s.	
Follistatin	962	883	n.s.	n.s.	
HGF	3155	2517	n.s.	n.s.	
IL-8	53	49	n.s.	n.s.	
G-CSF	892	810	n.s.	n.s.	
PDGF-BB	972	671	n.s.	n.s.	
VEGF	211	174	n.s.	n.s.	
Leptin	2623	3196	n.s.	n.s.	
PECAM-1	6159	5447	n.s.	n.s.	
IL-12	4	5	n.s.	n.s.	
FGF-basic	16	22	n.s.	n.s.	
TNF-α	4	4	n.s.	n.s.	

*Values indicate the average. Recurrence, post-operative recurrence; logistic, logistic regression model. The concentrations are ng/mL for interleukin 6 receptor (IL-6R), matrix metallopeptidase 9 (MMP-9), TIMP metallopeptidase inhibitor 1 (TIMP-1), TIMP-2, endostatin, P-selectin, intercellular adhesion molecule 1 (ICAM-1), vascular cell adhesion molecule 1 (VCAM-1), Tie-2, plasminogen activator inhibitor-1 (PAI-1), macrophage migration inhibitory factor (MIF), and plasminogen activator urokinase receptor (uPAR), and the others are pg/mL. FGF-basic, fibroblast growth factor 2; G-CSF, colony stimulating factor 3; HGF, hepatocyte growth factor; n.s., not significant; PDGF-BB, platelet-derived growth factor beta polypeptide; PECAM-1, platelet/endothelial cell adhesion molecule; TNF-α, tumor necrosis factor; VEGF, vascular endothelial growth factor.

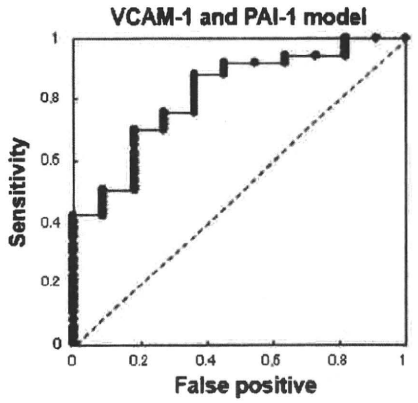

Fig. 2. The receiver–operator curve (ROC) for post-operative recurrence. A stepwise method selected vascular cell adhesion molecule 1 (VCAM-1) and plasminogen activator inhibitor-1 (PAI-1) as the most useful explanatory parameters; these two molecules were subsequently used to construct a prediction model. The ROC indicates the results of this model, which was capable of discriminating post-operative recurrence with an area under the curve (AUC) of 0.82, a sensitivity of 0.75, and a specificity of 0.73.

overexpressing the endothelial cell adhesion molecule VCAM-1, which normally mediates leukocyte extravasation to sites of tissue inflammation.[19]

Plasminogen activator inhibitor-1 (PAI-1)/SERPINE1 belongs to the plasmin/plasminogen system and is secreted into the blood, where it prevents the generation of plasmin, promoting the persistence and expansion of thrombi.[20] Plasminogen activator inhibitor-1 (PAI-1) is known as tumor biological prognostic factor and has been thoroughly validated with regard to its clinical utility in breast cancer.[21,22] The 2007 Breast Tumor Markers Guidelines recommend that uPA/PAI-1 be measured using an ELISA with a minimum of 300 mg of fresh or frozen breast cancer tissue for determining the prognosis of patients with newly diagnosed, node-negative breast cancer. Furthermore, CMF-based adjuvant chemotherapy provides a substantial benefit, compared with observation alone, in patients with a high risk of recurrence as determined by the presence of high levels of uPA and PAI-1.[23] Previous reports have demonstrated that higher levels of PAI-1, but not PAI-2, are associated with large tumors, metastatic stage, and a worse prognosis in patients with CRC.[24–26] Our study differed in that it evaluated the clinical parameter of post-operative recurrence in a prospective study. The biological mechanism by which PAI-1 promotes tumor progression is thought to involve a reduction in cell adhesion to the extracellular matrix as a consequence of excess PAI-1 interfering with uPAR binding to vitronectin, thereby facilitating cell invasion and migration.[27] Interestingly, accumulating data indicate that both VCAM-1 and PAI-1 promote tumor metastasis and cellular adhesion. These activities are likely involved in post-operative recurrence. We plan to perform

doi: 10.1111/j.1349-7006.2010.01595.x

a validation study to predict post-operative recurrence using the plasma concentrations of VCAM-1 and PAI-1 in the near future.

In conclusion, we have demonstrated that a combination prediction model based on the plasma concentrations of VCAM-1 and PAI-1 was a useful biomarker for predicting post-operative recurrence in patients with colorectal cancer. Our strategy, which utilizes a multiplex immunoassay system, may be a powerful tool for identifying biomarkers in clinical settings.

Acknowledgments

This study was supported by the Third-Term Comprehensive 10-Year Strategy for Cancer Control, a Grant-in-Aid for Scientific Research; the Program for the Promotion of Fundamental Studies in Health Sciences of the National Institute of Biomedical Innovation (NiBio); a Grant-in-Aid for Cancer Research (H20-20-9) from the Ministry of Health, Labour and Welfare; and a Grant-in-Aid for Scientific Research from the Ministry of Education, Culture, Sports, Science and Technology of Japan (19209018). The following people have played very important roles in the conduct of this project: Hiromi Orita, Hideko Morita, and Mari Araake.

Disclosure Statement

The authors have no conflict of interest.

References

1 Greenlee RT, Hill-Harmon MB, Murray T, Thun M. Cancer statistics, 2001. *CA Cancer J Clin* 2001; **51**: 15–36.

2 Ratto C, Sofo L, Ippoliti M, Merico M, Doglietto GB, Crucitti F. Prognostic factors in colorectal cancer. Literature review for clinical application. *Dis Colon Rectum* 1998; **41**: 1033–49.

3 Mutch MG. Molecular profiling and risk stratification of adenocarcinoma of the colon. *J Surg Oncol* 2007; **96**: 693–703.

4 Locker GY, Hamilton S, Harris J *et al.*; ASCO. ASCO 2006 update of recommendations for the use of tumor markers in gastrointestinal cancer. *J Clin Oncol* 2006;**24**:5313–27.

5 Park YJ, Park KJ, Park JG, Lee KU, Choe KJ, Kim JP. Prognostic factors in 2230 Korean colorectal cancer patients: analysis of consecutively operated cases. *World J Surg* 1999; **23**: 721–6.

6 Andreyev HJ, Norman AR, Cunningham D, Oates JR, Clarke PA. Kirsten ras mutations in patients with colorectal cancer: the multicenter "RASCAL" study. *J Natl Cancer Inst* 1998; **90**: 675–84.

7 Andreyev HJ, Norman AR, Cunningham D *et al.* Kirsten ras mutations in patients with colorectal cancer: the 'RASCAL II' study. *Br J Cancer* 2001; **85**: 692–6.

8 Popat S, Hubner R, Houlston RS. Systematic review of microsatellite instability and colorectal cancer prognosis. *J Clin Oncol* 2005; **23**: 609–18.

9 Aschele C, Debernardis D, Lonardi S *et al.* Deleted in colon cancer protein expression in colorectal cancer metastases: a major predictor of survival in patients with unresectable metastatic disease receiving palliative fluorouracil-based chemotherapy. *J Clin Oncol* 2004; **22**: 3758–65.

10 Duffy MJ, van Dalen A, Haglund C *et al.* Tumour markers in colorectal cancer: European Group on Tumour Markers (EGTM) guidelines for clinical use. *Eur J Cancer* 2007; **43**: 1348–60.

11 Kimura H, Kasahara K, Sekijima M, Tamura T, Nishio K. Plasma MIP-1beta levels and skin toxicity in Japanese non-small cell lung cancer patients treated with the EGFR-targeted tyrosine kinase inhibitor, gefitinib. *Lung Cancer* 2005; **50**: 393–9.

12 Galkina E, Ley K. Vascular adhesion molecules in atherosclerosis. *Arterioscler Thromb Vasc Biol* 2007; **27**: 2292–301.

13 Carter RA, Wicks IP. Vascular cell adhesion molecule 1 (CD106): a multifaceted regulator of joint inflammation. *Arthritis Rheum* 2001; **44**: 985–94.

14 Yao M, Huang Y, Shioi K *et al.* A three-gene expression signature model to predict clinical outcome of clear cell renal carcinoma. *Int J Cancer* 2008; **123**: 1126–32.

15 De Cicco C, Ravasi L, Zorzino L *et al.* Circulating levels of VCAM and MMP-2 may help identify patients with more aggressive prostate cancer. *Curr Cancer Drug Targets* 2008; **8**: 199–206.

16 Silva HC, Garcao F, Coutinho EC, De Oliveira CF, Regateiro FJ. Soluble VCAM-1 and E-selectin in breast cancer: relationship with staging and with the detection of circulating cancer cells. *Neoplasma* 2006; **53**: 538–43.

17 Shioi K, Komiya A, Hattori K *et al.* Vascular cell adhesion molecule 1 predicts cancer-free survival in clear cell renal carcinoma patients. *Clin Cancer Res* 2006; **12**: 7339–46.

18 Shariat SF, Karam JA, Walz J *et al.* Improved prediction of disease relapse after radical prostatectomy through a panel of preoperative blood-based biomarkers. *Clin Cancer Res* 2008; **14**: 3785–91.

19 Wu TC. The role of vascular cell adhesion molecule-1 in tumor immune evasion. *Cancer Res* 2007; **67**: 6003–6.

20 Durand MK, Bødker JS, Christensen A *et al.* Plasminogen activator inhibitor-I and tumour growth, invasion, and metastasis. *Thromb Haemost* 2004; **91**: 438–49.

21 Harbeck N, Schmitt M, Kates RE *et al.* Clinical utility of urokinase-type plasminogen activator and plasminogen activator inhibitor-1 determination in primary breast cancer tissue for individualized therapy concepts. *Clin Breast Cancer* 2002; **3**: 196–200.

22 Harbeck N, Kates RE, Schmitt M. Clinical relevance of invasion factors urokinase-type plasminogen activator and plasminogen activator inhibitor type 1 for individualized therapy decisions in primary breast cancer is greatest when used in combination. *J Clin Oncol* 2002; **20**: 1000–7.

23 Harris L, Fritsche H, Mennel R *et al.* American Society of Clinical Oncology, American Society of Clinical Oncology 2007 update of recommendations for the use of tumor markers in breast cancer. *J Clin Oncol* 2007; **25**: 5287–312.

24 Herszényi L, Plebani M, Carraro P *et al.* The role of cysteine and serine proteases in colorectal carcinoma. *Cancer* 1999; **86**: 1135–42.

25 Sier CF, Vloedgraven HJ, Ganesh S *et al.* Inactive urokinase and increased levels of its inhibitor type 1 in colorectal cancer liver metastasis. *Gastroenterology* 1994; **107**: 1449–56.

26 Langenskiöld M, Holmdahl L, Angenete E, Falk P, Nordgren S, Ivarsson ML. Differential prognostic impact of uPA and PAI-1 in colon and rectal cancer. *Tumour Biol* 2009; **30**(4): 210–20.

27 Berger DH, Plasmin/plasminogen system in colorectal cancer. *World J Surg* 2002; **26**: 767–71.

Supporting Information

Additional Supporting Information may be found in the online version of this article:

Fig. S1. Metastasis (+) *vs* (−) in independent samples of colorectal cancer (CRC) (n = 28).

Fig. S2. Post-operative recurrence (+) *vs* (−) in stage III colorectal cancer (CRC) (n = 45).

Please note: Wiley-Blackwell are not responsible for the content or functionality of any supporting materials supplied by the authors. Any queries (other than missing material) should be directed to the corresponding author for the article.

Gynecologic Oncology 118 (2010) 160–166

Contents lists available at ScienceDirect

Gynecologic Oncology

journal homepage: www.elsevier.com/locate/ygyno

Amplification of GNAS may be an independent, qualitative, and reproducible biomarker to predict progression-free survival in epithelial ovarian cancer

Ei-ichiro Tominaga [a], Hiroshi Tsuda [a,*], Tokuzo Arao [b], Sadako Nishimura [c], Masashi Takano [d], Fumio Kataoka [a], Hiroyuki Nomura [a], Akira Hirasawa [a], Daisuke Aoki [a], Kazuto Nishio [b]

[a] Department of Obstetrics and Gynecology, School of Medicine, Keio University Tokyo, Japan
[b] Department of Genome Biology, Kinki University School of Medicine, Osaka, Japan
[c] Department of Obstetrics and Gynecology, Osaka City General Hospital, Osaka, Japan
[d] Department of Obstetrics and Gynecology, National Defence Medical College, Tokorozawa, Japan

ARTICLE INFO

Article history:
Received 27 January 2010
Available online 26 May 2010

Keywords:
Ovarian cancer
Prognosis
Amplification
Biomarker
Carboplatin
Paclitexal

ABSTRACT

Objectives. The purpose of this study was to identify genes that predict progression-free survival (PFS) in advanced epithelial ovarian cancer (aEOC) receiving standard therapy.

Methods. We performed microarray analysis on laser microdissected aEOC cells. All cases received staging laparotomy and adjuvant chemotherapy (carboplatin + paclitaxel) as primary therapy.

Results. Microarray analysis identified 50 genes differentially expressed between tumors of patients with no evidence of disease (NED) or evidence of disease (ED) ($p<0.001$). Six genes (13%) were located at 8q24, and 9 genes (19.6%), at 20q11–13. The ratio of selected gene set/analyzed gene set in chromosomes 8 and 20 are significantly higher than that in other chromosome regions (6/606 vs. 32/13656, $p=0.01$) and (12/383 vs. 32/13656, $p=1.3\times10^{-16}$). We speculate that the abnormal chromosomal distribution is due to genomic alteration and that these genes may play an important role in aEOC and choose GNAS (GNAS complex locus, NM_000516) on 20q13 based on the p value and fold change. Genomic PCR of aEOC cells also showed that amplification of GNAS was significantly correlated with unfavorable PFS ($p=0.011$). Real-time quantitative RT-PCR analysis of independent samples revealed that high mRNA expression levels of the GNAS genes, located at chromosome 20q13, was significantly unfavorable indicators of progression-free survival (PFS). Finally, GNAS amplification was an independent prognostic factor for PFS.

Conclusions. Our results suggest that GNAS gene amplification may be an independent, qualitative, and reproducible biomarker of PFS in aEOC.

Introduction

Epithelial ovarian cancer (EOC) remains the most common cause of cancer death in women and the leading cause of death from gynecologic cancer. Early diagnosis of EOC is extremely difficult because most patients with early-stage disease are asymptomatic, so that 80% of patients present with advanced disease. Standard therapy includes surgical procedures (bilateral adnexectomy + hysterectomy + greater omentectomy) with staging laparotomy, debulking surgery, and postoperative chemotherapy using a combination of platinum and taxane. In 70% of advanced EOC (aEOC) patients, complete clinical responses are achieved; however, tumor recurs in most patients within 1 to 2 years after diagnosis and death is due to the development of chemotherapy resistance. In contrast, small numbers of patients with aEOC are cured by standard therapy. Although several clinical features are associated with poor prognosis, including poor performance status, suboptimal debulking surgery, clear cell or mucinous histology, high histologic grade, old age, or slow decrease in serum CA125 during adjuvant chemotherapy, reliable predictive biomarkers for aEOC are still lacking. If such markers could be established, patients who are likely to relapse and die of disease might be identified. These patients would be appropriate candidates for experimental approaches using novel anticancer drugs or new combination chemotherapy.

Recently, molecular diagnostic methods have been developed and BAX or BRCA1 have been reported to be predictive biomarker for aEOC [1,2]. We also previously reported that abnormalities of cell cycle regulators are predictive prognostic indicators for EOC [3]. Similarly, gene expression profiles or array comparative genomic hybridization (aCGH) has been reported to offer predictive/prognostic information for aEOC [4–7]. However, in order to identify useful predictive biomarkers for EOC, it is important that the markers should be tested in the context of standard therapy. In addition, the histology of the

* Corresponding author. Department of Obstetrics and Gynecology, School of Medicine, Keio University School of Medicine, 35 Shinanomachi, Shinjyuku-ku, Tokyo, 160-8582, Japan. Fax: +81 3 3353 0249.
E-mail address: htsud@sc.itc.keio.ac.jp (H. Tsuda).

0090-8258/$ – see front matter © 2010 Elsevier Inc. All rights reserved.
doi:10.1016/j.ygyno.2010.03.010

tumors should be considered because clear cell and mucinous types are usually more chemoresistant than other histologic types [3,9].

In this study, we used oligonucleotide microarrays combined with RNA isolated from microdissected tumor tissue to identify new prognostic biomarkers for aEOC patients receiving standard therapy. We excluded clear cell or mucinous tumors from our analysis based on the chemosensitivity.

Materials and methods

Patients and samples

Subjects eligible for this study were patients with histologically confirmed stage IIc–IV EOC (excluding mucinous and clear cell types) receiving standard therapy. Histologic grade was determined using WHO grading system. Additional inclusion criteria included an Eastern Cooperative Oncology Group performance status of 0 to 2. Exclusion criteria included a history of prior chemotherapy or major surgery. All patients received standard surgery and chemotherapy using carboplatin and paclitaxel. Standard surgery was bilateral adnexectomy, hysterectomy, and greater omentectomy with staging laparotomy and debulking surgery. Thirty-three aEOC patients were enrolled for microarray analysis, and an additional 107 patients were for real-time PCR analysis. The progression-free survival (PFS) was defined from the date of primary surgery to the date of the first occurrence of any of the following events: appearance of any new lesions, tumor progression, elevation of the CA125 level to at least two times the upper limit of normal or a nadir CA125 level, or death from any cause. The patients were determined to be no evidence of disease (NED) or evidence of disease (ED) at the disease progression or final visit. The study was approved by the Institutional Review Board of the Osaka City General Hospital and School of Medicine, Keio University, and written informed consent was obtained from all patients. Tumor specimens were obtained at operation and were immediately stored at −80 °C.

Study design

One hundred and forty aEOC samples were evaluated. The samples were divided between microarray analysis ($n = 33$) and a real-time PCR analysis ($n = 107$). Microarray analysis was performed using 33 samples, and candidate genes showing significant correlation with disease progression were identified. The GNAS gene was evaluated in an independent set of 107 samples, and PFS was predicted using the results of real-time PCR analyses of both mRNA and DNA.

Microdissection

Microdissection was performed as described previously. In brief, frozen sections (6 μm) prepared from tumor tissue specimens were affixed to glass slides and stained by Histogene LCM Frozen Section Staining Kit (Arcturus Engineering, Mountain View, CA). Stained sections were microdissected using a PixCell IIe LCM system (Arcturus Engineering, Mountain View, CA). Tumor cells and adjacent non-tumor stromal cells were visualized under the microscope and tumor cells selectively released by activation of the laser. Approximately 15,000 tumor cells were dissected in each case.

RNA and DNA extraction and amplification

Total RNA and DNA extractions were performed using the PicoPure RNA Isolation Kit and PicoPure DNA Extraction Kit according to the manufacturer's instructions (Arcturus Engineering, Mountain View, CA). RNA was amplified using a modified single-round T7 RNA amplification protocol. In brief, total RNA (600 ng) was first incubated with 1 μl of T7 primer(5′-GCATTAGCGGCCGCGAAATTAATACGACTCACTATAGGGAGATTTTTTTTTTTTTTTTTVN-3′, 200 ng/μl) in a total volume of 50 μl for 3 min at 70 °C. First-strand cDNA synthesis was then performed by incubating 5 μl of primer-annealed sample and 5 μl of first strand master mix containing 2 μl of 5× first-strand buffer, 1 μl of 0.1 M DTT, 0.5 μl of DEPC water, 0.5 μl 10 mM dNTP mix, 0.5 μl RNase inhibitor, and 0.5 μl of MMLV reverse transcriptase (200 U/μl) for 1 h and 15 min at 37 °C. Subsequently, second-strand cDNA synthesis was performed by incubating the 10 μl first-strand reaction with 65 μl of second master mix, which contained 46 μl DEPC water, 15 μl 5 × second-strand buffer, 1.5 μl of 10 mM dNTP mix, 0.5 μl of *Escherichia coli* DNA ligase (10 U/μl), 1.5 μl E. coli DNA polymerase I (10 U/μl), and 0.5 μl *E. coli* RNase H (2 U/μl), for 2 h at 16 °C, and then for 15 min at 70 °C. The entire 75 μl cDNA sample was loaded onto a ChromaSpin TE-200 spin column (BD Biosciences, San Diego, CA), which was centrifuged for 5 min at 2900 rpm (700×*g*) in an Eppendorf centrifuge. Purified cDNA was collected, lyophilized, dissolved in 8 μl of RNase-free water, and incubated at 70 °C for 10 min. In vitro transcription was subsequently performed by incubating the 8 μl post-lyophilization cDNA product with 12.2 μl of master mix containing 2 μl of 10× T7 reaction buffer, 6 μl of 25 mM rNTP Mix, 2 μl of 100 mM DTT, 0.2 μl of RNase inhibitor (40 U/ml), and 2 μl of T7 RNA polymerase for 3 h at 37 °C. The amplified RNA was purified on an RNeasy mini column (Qiagen, Valencia, CA) as per the manufacturer's protocol. The purified amplified RNA was quantified using RiboGreen RNA Quantitation Reagent (Molecular Probes, Eugene, OR).

Oligonucleotide microarray analysis

The microarray procedure was performed according to Affymetrix protocols (Santa Clara, CA). In brief, total RNA extracted from tumor samples was checked for quality using an Agilent 2100 Bioanalyzer (Agilent Technologies, Waldbronn, Germany) and cRNA was synthesized using the GeneChip 3′-Amplification Reagents One-Cycle cDNA Synthesis Kit (Affymetrix). The labeled cRNAs were then purified and used for construction of probes. Hybridization was performed using the Affymetrix GeneChip HG-U133 Plus2.0 array for 16 h at 45 °C. Signal intensities were measured using a GeneChip Scanner3000 (Affymetrix) and converted to numerical data using the GeneChip Operating Software, Ver.1 (Affymetrix).

DNA copy number analysis

The method has been described previously [5,10]. From array data, we focused on 20q11–13 loci for further examination, because we thought that 20q11–13 loci are amplified in the ED group. We chose GNAS (GNAS complex locus, NM_000516) on 20q13 based on the *p* value and fold change. Results were normalized to the amount of RH78455 of chromosome 5q22.2 as genomic internal control locus. Regarding the internal DNA copy number control, we selected the genomic region of chromosome 5q, which is less frequently received the genomic alterations in ovarian cancers referred to previous report [11–13]. Next, we checked 10 primers (D5S818, D5S409, D5S349, D5S346, D5S519, D5S422, STSR33609, RH46186, RH78455, RH68508) of chromosome 5 region according to database of sequence tagged sites (STSs, http://www.ncbi.nlm.nih.gov/unists). Among them, RH78455 was most specific and reproducible primers, then we used it as internal DNA copy number control. The DNA was quantified using the Power SYBR Green PCR Master Mix (Applied Biosystems) and 7900HT Fast Real-time PCR system (Applied Biosystems) and reported relative to the control primer. The control DNA for standard DNA copy numbers was purchased from Invitrogen (Carlsbad, CA). The PCR conditions were as follows: one cycle of denaturation at 95 °C for 10 min, followed by 40 cycles at 95 °C for 15 s and 60 °C for 60 s. If copy number was >1.5 relative to the chromosome control, we judged that there was amplification [5]. The primers used for estimating DNA copy numbers were as follows: GNAS: SHGC59923-FW: 5-GGG TGG GCT TTT GTT CTT TG-3, SHGC59923-RW: 5-AGG CAT AAA CGG GGG AGA TT-3, and

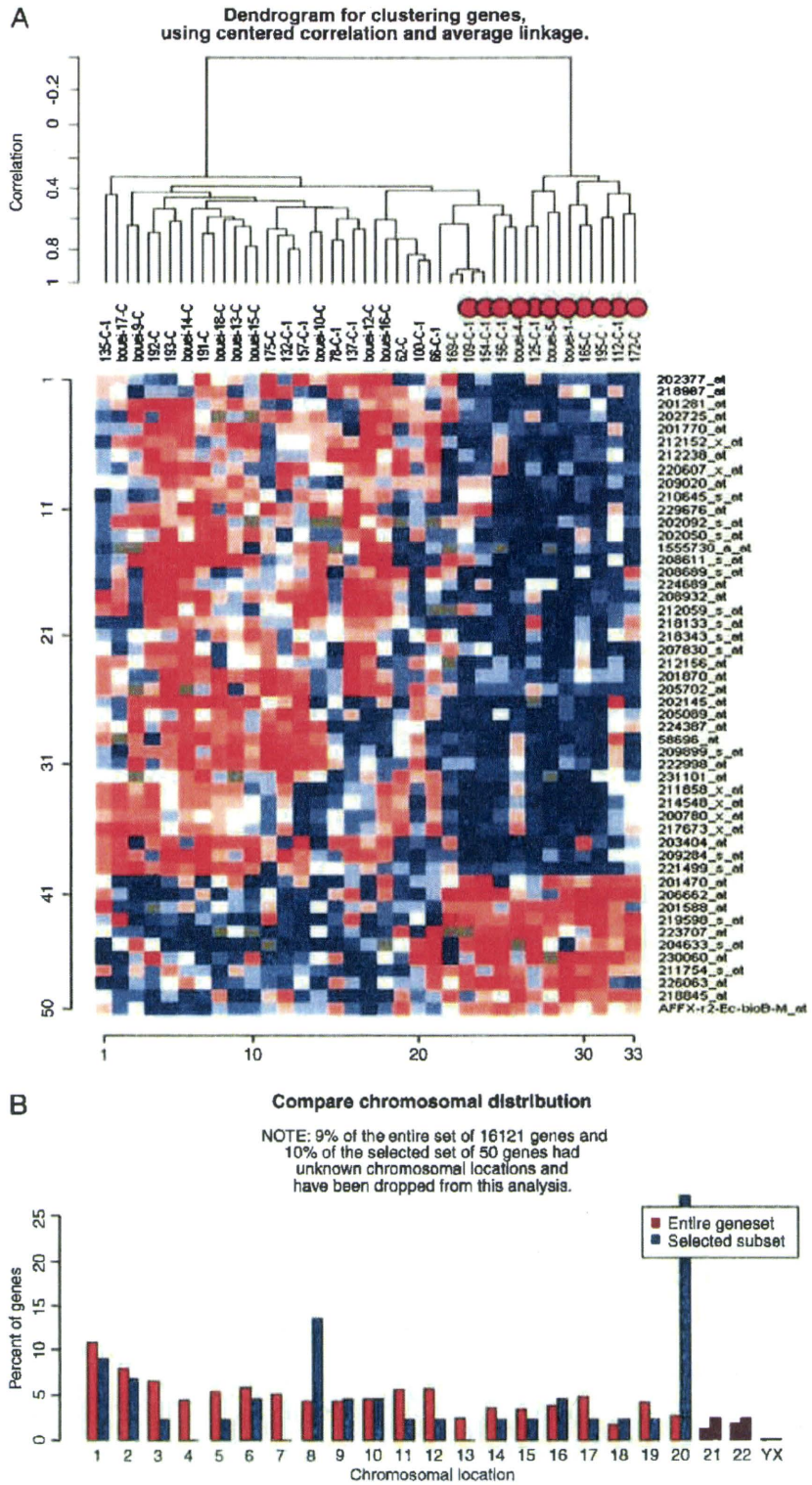

Fig. 1. (A) Fifty genes differentially expressed between tumors in ED and NED patients. Dendrogram for clustering genes using centered correlation and average linkage. Red circles indicate NED cases. (B) The chromosome distribution of the entire gene set and the selected subset of 50 genes. Among genes, which are located on chromosome 8 and 20, 50 genes are frequently selected in aEOC.

Table 1
Identification of 50 candidate PFS-related genes from microarray analysis.

No.	Name	Symbol	Cytoband	Fold Difference	Probe Set
1	Zinc finger, MYM-type 4	ZMYM4	Chr:1p32-p34	1.6	202050_s_at
2	Putative homeodomain transcription factor 1	PHTF1	Chr:1p13	1.5	205702_at
3	Protein phosphatase 1, regulatory (inhibitor) subunit 8	PPP1R8	Chr:1p35	1.8	207830_s_at
4	AT-rich interactive domain 1A (SWI-like)	ARID1A	Chr:1p35.3	1.8	212152_x_at
5	NIF3 NGG1 interacting factor 3-like 1 (S. pombe)	NIF3L1	Chr:2q33	1.6	218133_s_at
6	General transcription factor IIIC, polypeptide3, 102 kDa	GTF3C3	Chr:2q33.1	1.5	218343_s_at
7	Cell division cycle associated 7	CDCA7	Chr:2q31	0.4	230060_at
8	Chromosome 3 open reading frame 63	C3orf63	Chr:3p14.3	1.9	209284_s_at
9	Glutaredoxin (thioltransferase)	GLRX	Chr:5q14	0.3	206662_at
10	Dual specificity phosphatase 22	DUSP22	Chr:6p25.3	0.5	218845_at
11	RWD domain containing 1	RWDD1	Chr:6q13-q22.33	0.5	219598_s_at
12	Lymphocyte antigen 6 complex, locus E	LY6E	Chr:8q24.3	3	202145_at
13	Zinc finger protein 7	ZNF7	Chr:8q24	1.6	205089_at
14	Fuse-binding protein-interacting repressor	SIAHBP1	Chr:8q24.2-qter	1.8	209899_s_at
15	MAF1 homolog (S. cerevisiae)	MAF1	Chr:8q24.3	1.8	222998_at
16	COMM domain containing 5//COMM domain containing 5	COMMD5	Chr:8q24-qter	1.8	224387_at
17	Exosome component 4	EXOSC4	Chr:8q24.3	1.7	58696_at
18	Spectrin, alpha, non-erythrocytic 1 (alpha-fodrin)	SPTAN1	Chr:9q33-q34	2	208611_s_at
19	vav 2 oncogene	VAV2	Chr:9q34.1	0.6	226063_at
20	Glutathione S-transferase omega 1	GSTO1	Chr:10q25.1	0.6	201470_at
21	PAP-associated domain containing 1	PAPD1	Chr:10p11.23	1.8	229676_at
22	Cofilin 1 (non-muscle)	CFL1	Chr:11q13	2.4	1555730_a_at
23	Activating transcription factor 7 interacting protein	ATF7IP	Chr:12p13.1	1.6	218987_at
24	Ribosomal protein S6 kinase, 90 kDa, polypeptide 5	RPS6KA5	Chr:14q31-q32.1	0.5	204633_s_at
25	Vacuolar protein sorting 39 (yeast)	VPS39	Chr:15q15.1	1.6	212156_at
26	ADP-ribosylation factor-like 2 binding protein	ARL2BP	Chr:16q13	1.5	202092_s_at
27	Protein phosphatase 4 (formerly X), catalytic subunit	PPP4C	Chr:16p12-16p11	1.9	208932_at
28	Polymerase (RNA) II (DNA-directed) polypeptide A, 220 kDa	POLR2A	Chr:17p13.1	1.8	202725_at
29	Thioredoxin-like 1	TXNL1	Chr:18q21.31	0.6	201588_at
30	Small nuclear ribonucleoprotein polypeptide A	SNRPA	Chr:19q13.1	1.7	201770_at
31	GNAS complex locus	GNAS	Chr:20q13.3	1.4	200780_x_at
32	Adhesion regulating molecule 1	ADRM1	Chr:20q13.33	1.6	201281_at
33	Ribophorin II	RPN2	Chr:20q12-q13.1	1.9	208689_s_at
34	Chromosome 20 open reading frame 111	C20orf111	Chr:20q13.11	1.5	209020_at
35	GNAS complex locus	GNAS	Chr:20q13.3	1.9	211858_x_at
36	Transient receptor potential cation channel, subfamily C, member 4-associated protein	TRPC4AP	Chr:20q11.22	1.7	212059_s_at
37	Additional sex combs like 1 (Drosophila)	ASXL1	Chr:20q11.1	1.7	212238_at
38	GNAS complex locus	GNAS	Chr:20q13.3	1.8	214548_x_at
39	GNAS complex locus	GNAS	Chr:20q13.3	1.6	217673_x_at
40	TH1-like (Drosophila)	TH1L	Chr:20q13	1.7	220607_x_at
41	Ayntaxin 16	STX16	Chr:20q13.32	1.7	221499_s_at
42	Mannosidase, beta A, lysosomal-like	MANBAL	Chr:20q11.23-q12	1.5	224689_at
43	Tetratricopeptide repeat domain 3	TTC3	Chr:21q22.2	1.5	210645_s_at
44	Solute carrier family 25 (mitochondrial carrier; peroxisomal membrane protein, 34 kDa), member 17	SLC25A17	Chr:22q13.2	0.6	211754_s_at
45	Translocase of outer mitochondrial membrane 34	TOMM34		1.6	201870_at
46				1.7	202377_at
47	Hypothetical protein MGC10850	MGC10850		0.5	223707_at
48	Transcribed locus			1.6	231101_at
49	Armadillo repeat containing, X-linked 2	ARMCX2	Chr:Xq21.33-q22.2	2.8	203404_at
50				0.7	AFFX-r2-Ec-bioB-M_at

chromosome 5q22.2: RH78455-FW: 5-TCC TGC AAA CAT TTA AAC TCC A-3, RH78455-RW: 5-AAC AGC AAC TGT TTT TTC CCC-3. Finally, for PCR, 1.5-fold was used as the cutoff for amplification, respectively [5].

Real-time quantitative RT-PCR for mRNA expression

In addition, mRNA expression levels were validated for GNAS (GNAS complex locus, NM_000516) on chromosome 20q13. All results were normalized to the amount of glyceraldehyde 3 phosphate dehydrogenase (GAPD, NM_002046). RNA was converted to cDNA using a GeneAmp RNA PCR Core kit (Applied Biosystems, Foster City, CA). The cDNAs were quantified using the Power SYBR Green PCR Master Mix (Applied Biosystems) and 7900HT Fast Real-time PCR system (Applied Biosystems) and reported relative to the GAPD expression levels. The PCR conditions were as follows: one cycle of denaturation at 95 °C for 10 min, followed by 40 cycles at 95 °C for 15 s, and 60 °C for 60 s. To amplify the target genes, all of the primers used for real-time RT-PCR were purchased from Takara (Yotsukaichi, Japan), which is the major company of molecular biology in Japan. We are frequently using their primers [14–16], and we consider that the primers are reliable one. GNAS-FW: 5-TGT ACA AGC AGT TAA TCA CCC ACC A-3, RW: 5-TCT GTA GGC CGC CTT AAG CTT TC-3, GAPD-FW: 5-GCA CCG TCA AGG CTG AGA AC-3, RW: 5-ATG GTG GTG AAG ACG CCA GT-3. Finally, we determined the case as overexpression when the relative mRNA expression is larger than median relative mRNA expression in all cases.

Statistical analysis

The microarray analysis was performed using the BRB Array Tools software ver. 3.3.0 (http://www.linus.nci.nih.gov/BRB-ArrayTools.html) developed by Dr. Richard Simon and Dr. Amy Peng. In brief, a log base 2 transformation was applied to the raw microarray data, and global normalization was used to calculate the median over the entire array. Genes were excluded if the percentage of data missing or filtered out exceeded 20% or if less than 20 % of expression data had at least a 1.5-fold change in either direction from the median value.

The 16,121 genes that passed the filtering criteria were then considered for further analysis. The *t*-test ($p<0.001$) was used to identify the genes differentially expressed between NED and ED. Clustering for 50 identified genes used centered correlation and average linkage.

Both mRNA and DNA copy numbers were validated using real-time PCR in the 107 independent cases of EOC. PFS was calculated by the Kaplan-Meier method. Univariate and multivariate Cox's proportional hazard test was applied to identify variables associated with PFS. A p value of <0.05 was considered to be significant (SAS software ver. 9.1.3; SAS Institute Inc., Cary, NC).

Results

Clinical backgrounds of 140 EOC

The clinical backgrounds of the 33 aEOC samples used for array analysis are as follows: median age (54 years: range 33–80), stage (II:4, III:19, IV:10), histologic types (endometrioid: 4, serous: 22, undifferentiated: 7), histologic grade (1+2:9, 3:24), and operation status (optimal:14, suboptimal:19). The median follow-up period is 907 days (range: 292–2136 days), and 11 patients are alive without relapse.

The clinical backgrounds of 107 aEOC samples assayed for real-time PCR are as follows: median age (54 years: range 29–85), stage (II:12, III:74, IV:21), histologic types (endometrioid: 27, serous: 61, undifferentiated: 19), histologic grade (1+2:46, 3:61), operation status (optimal: 61, suboptimal: 46). The median follow-up period is 699 days (range: 92–2885 days) and 49 patients are alive without relapse.

Identification of 50 candidate disease progression-related genes by microarray analysis

To identify candidate disease progression-related genes from 54,675 transcripts, microarray analysis was performed on a training set of 33 samples. A total of 16,121 genes passed the filtering criteria and were further analyzed. Fifty genes were significantly correlated with disease progression, with a p value of <0.001 (Fig. 1A, Table 1). The chromosome distribution of the gene set analyzed and a selected subset are shown in Fig. 1B. Fifty selected genes on chromosome 8 and 20 show a higher than expected chromosomal distribution (Fig. 1B). Of these 50 genes, 6 are located at chromosome 8q24 and 9 (12 probes) at 20q11–13. The ratio of selected gene set/analyzed gene set in chromosome 20 is significantly higher than that in other chromosome regions (12/383 vs. 32/13656, $p=1.3\times10^{-16}$) and the selected gene set/analyzed gene set in chromosome 8 is significantly higher than that in other chromosome regions (6/606 vs. 32/13656, $p=0.01$). We speculate that the abnormal chromosomal distribution is due to genomic alteration and that these genes may play an important role in aEOC.

The results suggested that 8q24 and 20q11–13 loci are amplified in the ED group and that this might be related to treatment of aEOC.

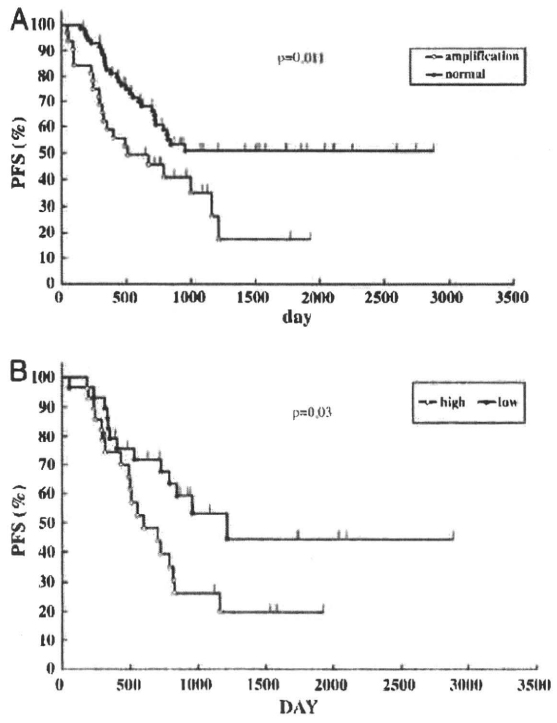

Fig. 2. The relationship between amplification and expression status of GNAS and PFS. (A) The relationship between copy number change of GNAS and PFS. (B) The relationship between mRNA expression of GNAS and PFS.

Table 2
Relationship between gene amplification and clinical factors.

Clinical Factor	GNAS	
	Frequency	*p* Value
Age		
Young	30%(16/53)	0.999
Old	30%(16/53)	
Grade		
1+2	33%(15/45)	0.689
3	28%(17/61)	
Operation		
Optimal	26%(16/61)	0.392
Suboptimal	36%(16/45)	

Relationship between GNAS gene amplification and PFS

DNA marker is thought to be more reliable and qualitative than RNA, because RNA expression changes according to the condition and environment of cancer cells. Therefore, we focused on detecting genomic alterations of chromosome 20q11–13 loci using real-time quantitative PCR on the 107 independent validation samples. The amplification of GNAS is significantly related to poor PFS ($p=0.011$) (Fig. 2A). GNAS shows gain of gene copy number rates of 30% (32/106), respectively. Correlations between amplification of GNAS and clinical factors are shown in Table 2. There are no significant associations between gene amplification at this loci and clinical factors such as age, histological grade, histologic type, and operation status. In addition, we performed multivariate Cox's proportional hazard test to identify variables including age, histologic grade, debulking status, histologic type, and GNAS copy number change associated with PFS. Finally, GNAS amplification was independent prognostic factor in aEOC (Table 3).

Table 3
Univariate and multivariate analysis of the effect of various prognostic factors on PFS.

Variable[a]	Univariate			Multivariate		
	Hazards Ratio[b]	95% CI	*p*	Hazards Ratio[b]	95% CI	*p*
GNAS	2.035	1.164–3.558	0.013	1.906	1.081–3.36	0.026
Age	0.975	0.563–1.688	0.927	0.765	0.434–1.348	0.354
Histologic grade	1.376	0.774–2.447	0.277	1.248	0.697–2.233	0.22
Debulking status	0.26	0.143–0.471	<0.001	0.256	0.139–0.493	<0.001

[a] GNAS: amplification vs. non-amplification, AGE: >median vs, ≤median, histologic grade: G3 vs. G1 + 2, debulking status: optimal vs. suboptimal.

[b] Hazard ratio refers to risk of survival, with values <1.0 indicating reduced risk. CI, confidence interval.

Relationship between GNAS gene expression and PFS

Of the 107 independent samples, RNA from 62 was available for real-time RT-PCR analysis. There are no significant associations between GNAS expression and clinical factors such as age, histological grade, and operation status. GNAS expression correlates significantly with PFS of aEOC ($p = 0.03$) (Fig. 2B).

Discussion

The platinum/taxane regimen has improved the prognosis of EOC; however, this remains poor. For this reason, it is very important to find new prognostic markers for EOC receiving standard therapy, so that future clinical trials can be focused on patients with a poor prognosis. In this study, we used oligonucleotide microarrays to identify new prognostic biomarkers for aEOC excluding clear cell or mucinous types receiving standard therapy. In the past decade, several studies have analyzed chromosomal imbalances using comparative genomic hybridization (CGH) in EOC [10,17–20]. Arnold et al. investigated 47 malignant ovarian tumors and 2 ovarian tumors of low malignant potential using CGH and demonstrated that common genetic changes include DNA gains of chromosome arms 8q24 (51%) and 20q13.2-qter (40%) [10]. Iwabuchi et al. presented CGH data from 31 ovarian carcinomas and reported that increased copy numbers were most commonly observed in their cases at 3q26 (42%), 8q24 (35%), and 12q11.1–12 (25%) [17], while Sonoda et al. demonstrated that the most frequent sites of copy number increase were 8q24.1 (56%) and 20q13.2-qter (48%) in tumor DNA from 25 malignant ovarian carcinomas and 2 tumors of low malignant potential [18]. Tanner et al. focused on 20q12–q13 amplification in 24 sporadic, 3 familial and 4 hereditary ovarian carcinomas, and 8 ovarian cancer cell lines [19]. They demonstrated high-level amplification of at least one of the five non-syntenic regions at 20q12–q13.2 in 13 sporadic (54%) and in all four hereditary tumors [19]. Hu et al. focused on ovarian serous carcinomas and demonstrated DNA copy number gain at 8q22q24 and 20q12q13 in 60% and 45% of samples, respectively [20] In our study, amplification rates of GNAS at 20q13 is 30%, respectively.

Furthermore, Tanner et al. showed a tendency toward correlation between amplification and poor survival (not significant) and Hu et al. reported that 20q12q13 amplification may indicate a high risk for recurrence of serous ovarian cancer [19,20]. These reports included various histologic types and stages and even cell lines as well as primary and recurrent cases. Furthermore, they provide no information on therapy or operation status, include small number of patients, and do not perform validation assays. As it is well established that patients with ovarian carcinoma of different histologic types vary in their response to chemotherapy [8,9], it is important to take this into account in testing new biomarkers for their utility in clinical practice. In this study therefore, we focused on patients receiving standard therapy, excluding those with mucinous and clear cell tumors, and performed microarray analysis in 33 patients and validation assays in 107 patients.

Recent attempts to develop accurate predictors of clinical outcome in ovarian cancer have focused on techniques that are capable of assessing global gene status such as expression profiling and array CGH [4–7]. Birrer et al. performed oligonucleotide array CGH on 42 microdissected high-grade serous ovarian tumors and reported that amplification at 5q31–5q35.3 exhibited the strongest correlation with overall survival, identifying FGF-1 on 5q31 as a prognostic marker in 81 independent samples [7]. These data are not in agreement with our own. However, Birrer et al.'s report provides no information about the chemotherapy used, so that we speculate that prognostic biomarkers may be dependent on the chemotherapeutic regimen. Spentzos et al. also reported expression profiles for EOC and established a Chemotherapy Response Profile (CRP) and Ovarian Cancer Prognostic Profile (OCPP) [4,6].

We selected GNAS gene based on the p value and fold change in array data and examined the amplification status of GNAS as prognostic marker of aEOC. GNAS gene amplification was an independent prognostic factor. The GNAS locus encodes the G (alpha) protein, which stimulates the formation of cyclic AMP (cAMP). The cAMP pathway mediates pleiotropic effects including regulation of apoptosis and proliferation [21–23] and different genotypes of the single nucleotide polymorphism (ANP) T393C in the GNAS gene predict the clinical outcome of urothelial carcinoma, sporadic colorectal cancer, renal cell carcinoma, and chronic lymphocytic leukemia [24–27]. However, the role of GNAS in EOC remains unclear.

In conclusion, we identified amplification of GNAS on 20q13 as markers of prognosis in patients with aEOC treated with standard therapy. Our finding identifies qualitative and reproducible biomarker to predict the PFS of aEOC.

Conflict of interest statement

All of the authors are aware of and agree to the content of the article and have no conflict interest.

Acknowledgments

The authors are grateful to Asami Nagata, Kanako Matsumoto, and Nozomi Tsuji for their technical assistance. This study was supported in part by a Grant-in-Aid for Scientific Research on Priority Areas from the Ministry of Education, Science and Culture, Japan (20014024), A Grant-in Aid for scientific Research (C) from the Ministry of Education, Science and Culture, Japan (19591940), and a grant from Osaka City General Hospital.

References

[1] Ben David Y, Chetrit A, Hirsh-Yechezkel G, Friedman E, Beck BD, Beller U, et al. Effect of BRCA mutations on the length of survival in epithelial ovarian tumors. J Clin Oncol 2002;20(2):463–6.
[2] Tai YT, Lee S, Niloff E, Weisman C, Strobel T, Cannistra SA. BAX protein expression and clinical outcome in epithelial ovarian cancer. J Clin Oncol 1998;16(8):2583–90.
[3] Kusume T, Tsuda H, Kawabata M, Inoue T, Umesaki N, Suzuki T, et al. The p16-cyclin D1/CDK4-pRb pathway and clinical outcome in epithelial ovarian cancer. Clin Cancer Res 1999;5(12):4152–7.
[4] Spentzos D, Levine DA, Ramoni MF, Joseph M, Gu X, Boyd J, et al. Gene expression signature with independent prognostic significance in epithelial ovarian cancer. J Clin Oncol 2004;22(23):4700–10.
[5] Tsuda H, Ito YM, Ohashi Y, Wong KK, Hashiguchi Y, Welch WR, et al. Identification of overexpression and amplification of ABCF2 in clear cell ovarian adenocarcinomas by cDNA microarray analyses. Clin Cancer Res 2005;11(19 Pt 1):6880–8.
[6] Spentzos D, Levine DA, Kolia S, Otu H, Boyd J, Libermann TA, et al. Unique gene expression profile based on pathologic response in epithelial ovarian cancer. J Clin Oncol 2005;23(31):7911–8.
[7] Birrer MJ, Johnson ME, Hao K, Wong KK, Park DC, Bell A, et al. Whole genome oligonucleotide-based array comparative genomic hybridization analysis identified fibroblast growth factor 1 as a prognostic marker for advanced-stage serous ovarian adenocarcinomas. J Clin Oncol 2007;25(16):2281–7.
[8] Takano M, Kikuchi Y, Yaegashi N, Kuzuya K, Ueki M, Tsuda H, et al. Clear cell carcinoma of the ovary: a retrospective multicentre experience of 254 patients with complete surgical staging. Br J Cancer 2006;94(10):1369–74.
[9] Hess V, A'Hern R, Nasiri N, King DM, Blake PR, Barton DP, et al. Mucinous epithelial ovarian cancer: a separate entity requiring specific treatment. J Clin Oncol 2004;22(6):1040–4.
[10] Arnold N, Hagele L, Walz L, Schempp W, Pfisterer J, Bauknecht T, et al. Overrepresentation of 3q and 8q material and loss of 18q material are recurrent findings in advanced human ovarian cancer. Genes Chromosom Cancer 1996;16(1):46–54.
[11] Mayr D, Kanitz V, Anderegg B, Luthardt B, Engel J, Lohrs U, et al. Analysis of gene amplification and prognostic markers in ovarian cancer using comparative genomic hybridization for microarrays and immunohistochemical analysis for tissue microarrays. Am J Clin Pathol 2006;126(1):101–9.
[12] Israeli O, Gotlieb WH, Friedman E, Korach J, Goldman B, Zeltser A, et al. Genomic analyses of primary and metastatic serous epithelial ovarian cancer. Cancer Genet Cytogenet 2004;154(1):16–21.
[13] Schipf A, Mayr D, Kirchner T, Diebold J. Molecular genetic aberrations of ovarian and uterine carcinosarcomas—a CGH and FISH study. Virchows Arch 2008;452(3):259–68.
[14] Kaneda H, Arao T, Tanaka K, Tamura D, Aomatsu K, Kudo K, et al. FOXQ1 is overexpressed in colorectal cancer and enhances tumorigenicity and tumor growth. Cancer Res;70(5):2053–2063.

[15] Matsumoto K, Arao T, Tanaka K, Kaneda H, Kudo K, Fujita Y, et al. mTOR signal and hypoxia-inducible factor-1 alpha regulate CD133 expression in cancer cells. Cancer Res 2009;69(18):7160–4.
[16] Tanaka K, Arao T, Maegawa M, Matsumoto K, Kaneda H, Kudo K, et al. SRPX2 is overexpressed in gastric cancer and promotes cellular migration and adhesion. Int J Cancer 2009;124(5):1072–80.
[17] Iwabuchi H, Sakamoto M, Sakunaga H, Ma YY, Carcangiu ML, Pinkel D, et al. Genetic analysis of benign, low-grade, and high-grade ovarian tumors. Cancer Res 1995;55(24):6172–80.
[18] Sonoda G, Palazzo J, du Manoir S, Godwin AK, Feder M, Yakushiji M, et al. Comparative genomic hybridization detects frequent overrepresentation of chromosomal material from 3q26, 8q24, and 20q13 in human ovarian carcinomas. Genes Chromosom Cancer 1997;20(4):320–8.
[19] Tanner MM, Grenman S, Koul A, Johannsson O, Meltzer P, Pejovic T, et al. Frequent amplification of chromosomal region 20q12-q13 in ovarian cancer. Clin Cancer Res 2000;6(5):1833–9.
[20] Hu J, Khanna V, Jones MW, Surti U. Comparative study of primary and recurrent ovarian serous carcinomas: comparative genomic hybridization analysis with a potential application for prognosis. Gynecol Oncol 2003;89(3):369–75.
[21] Srivastava RK, Srivastave AR, Cho-Chung YS. Synergistic effects of 8-Cl-cAMP and retinoic acids in the inhibition of growth and induction of apoptosis in ovarian cancer cells: induction of retinoic acid receptor beta. Mol Cell Biochem 2000;204 (1–2):1–9.
[22] Yan L, Herrmann V, Hofer JK, Insel PA. beta-adrenergic receptor/cAMP-mediated signaling and apoptosis of S49 lymphoma cells. Am J Physiol Cell Physiol 2000;279 (5):C1665–74.
[23] Wu EH, Tam BH, Wong YH. Constitutively active alpha subunits of G(q/11) and G (12/13) families inhibit activation of the pro-survival Akt signaling cascade. FEBS J 2006;273(11):2388–98.
[24] Frey UH, Alakus H, Wohlschlaeger J, Schmitz KJ, Winde G, van Calker HG, et al. GNAS1 T393C polymorphism and survival in patients with sporadic colorectal cancer. Clin Cancer Res 2005;11(14):5071–7.
[25] Frey UH, Eisenhardt A, Lummen G, Rubben H, Jockel KH, Schmid KW, et al. The T393C polymorphism of the G alpha s gene (GNAS1) is a novel prognostic marker in bladder cancer. Cancer Epidemiol Biomarkers Prev 2005;14(4): 871–7.
[26] Frey UH, Lummen G, Jager T, Jockel KH, Schmid KW, Rubben H, et al. The GNAS1 T393C polymorphism predicts survival in patients with clear cell renal cell carcinoma. Clin Cancer Res 2006;12(3 Pt 1):759–63.
[27] Frey UH, Nuckel H, Sellmann L, Siemer D, Kuppers R, Durig J, et al. The GNAS1 T393C polymorphism is associated with disease progression and survival in chronic lymphocytic leukemia. Clin Cancer Res 2006;12(19):5686–92.

Int J Clin Oncol
DOI 10.1007/s10147-010-0170-6

ORIGINAL ARTICLE

High-dose dexamethasone plus antihistamine prevents colorectal cancer patients treated with modified FOLFOX6 from hypersensitivity reactions induced by oxaliplatin

Yasuhiro Kidera · Taroh Satoh · Shinya Ueda · Wataru Okamoto · Isamu Okamoto · Soichi Fumita · Kimio Yonesaka · Hidetoshi Hayashi · Chihiro Makimura · Kunio Okamoto · Hidemi Kiyota · Junji Tsurutani · Masaki Miyazaki · Masahiro Yoshinaga · Kimiko Fujiwara · Yuzuru Yamazoe · Kenzo Moriyama · Masanobu Tsubaki · Yasutaka Chiba · Shozo Nishida · Kazuhiko Nakagawa

Received: 4 September 2010 / Accepted: 29 November 2010

Abstract
Background Oxaliplatin is a third-generation platinum compound and a key agent for the management of colorectal cancer. Patients treated with oxaliplatin are at risk for hypersensitivity reactions. We designed a modified premedication regimen to prevent oxaliplatin-related hypersensitivity reactions and assessed if this approach is effective.
Methods A retrospective cohort study of patients with advanced colorectal cancer who received modified FOLFOX6 (mFOLFOX6) was performed. Patients received routine premedication with dexamethasone 8 mg and granisetron 3 mg for the first five cycles of mFOLFOX6. From the sixth cycle onward, cohort 1 received the same premedication, and cohort 2 received modified premedication (diphenhydramine 50 mg orally, followed by dexamethasone 20 mg, granisetron 3 mg, and famotidine 20 mg). We compared the incidence of hypersensitivity reactions, duration of treatment, and reasons for treatment withdrawal between the two cohorts.
Results A total of 181 patients were studied (cohort 1, 81; cohort 2, 100). Hypersensitivity reactions developed in 16 patients (20%) in cohort 1 and 7 (7.0%) in cohort 2 ($P = 0.0153$). The median number of cycles increased from 9 in cohort 1 to 12 in cohort 2. Apart from progressive disease, neurotoxicity was the reason for discontinuing treatment in 20% of the patients in cohort 1, as compared with 53% in cohort 2.
Conclusion Increased doses of dexamethasone and antihistamine significantly reduced oxaliplatin-related hypersensitivity reactions. This effective approach should be considered for all patients who receive FOLFOX, allowing treatment to be completed as planned.

Keywords Colorectal cancer · FOLFOX · Hypersensitivity reaction · Oxaliplatin · Premedication

Y. Kidera · M. Tsubaki · S. Nishida
Division of Pharmacotherapy,
Kinki University School of Pharmacy,
3-4-1 Kowakae, Higashi-Osaka, Osaka 577-8502, Japan

Y. Kidera · M. Yoshinaga · K. Fujiwara · Y. Yamazoe · K. Moriyama
Department of Pharmacy, Kinki University School of Medicine, 377-2 Ohno-higashi, Osaka-Sayama, Osaka 589-8511, Japan

T. Satoh (✉) · S. Ueda · W. Okamoto · I. Okamoto · S. Fumita · K. Yonesaka · H. Hayashi · C. Makimura · K. Okamoto · H. Kiyota · J. Tsurutani · M. Miyazaki · K. Nakagawa
Department of Medical Oncology, Kinki University School of Medicine, 377-2 Ohno-higashi, Osaka-Sayama, Osaka 589-8511, Japan
e-mail: taroh@med.kindai.ac.jp

Y. Chiba
Department of Environmental Medicine and Behavioral Science, Kinki University School of Medicine, 377-2 Ohno-higashi, Osaka-Sayama, Osaka 589-8511, Japan

Introduction

Oxaliplatin, a third-generation platinum derivative, in combination with fluorouracil and leucovorin (FOLFOX) is among the most effective chemotherapies for metastatic colorectal cancer. The increasing use of oxaliplatin for chemotherapy has led to an increased incidence of oxaliplatin-related hypersensitivity reactions. The MOSAIC trial, in which more than 1,100 patients with colorectal cancer received 5-fluorouracil with oxaliplatin in an adjuvant setting, reported a 10.3% incidence of hypersensitivity reactions, which were one of the major reasons for discontinuing treatment [1].

Published online: 18 January 2011

Hypersensitivity is defined as an unexpected reaction inconsistent with a drug's usual toxicity profile. Such reactions usually occur during or immediately after treatment. Once sensitized, patients have recurrent hypersensitivity reactions on subsequent exposure to oxaliplatin. Desensitization protocols have been designed to prevent hypersensitivity reactions. Such protocols have allowed successful rechallenge with oxaliplatin [2, 3]. However, clinical criteria for rechallenge with oxaliplatin remain a matter of debate. Reliable methods for predicting the risk of severe hypersensitivity reactions to oxaliplatin have not been established. The potential risks of rechallenge with oxaliplatin after severe anaphylaxis should be weighed against the expected benefits according to the specific clinical situation.

Hypersensitivity reactions to platinum salts (cisplatin, carboplatin) are classically type I (i.e., immediate) reactions [4], the incidence of which increases with multiple cycles of therapy [5]. The symptoms can resolve after treatment with antihistamines and steroids. More recent series have documented a considerably higher incidence of hypersensitivity reactions, ranging between 8% and 19% [6–10]. Besides these reports, studies assessing the preventative effect of premedication on oxaliplatin-related hypersensitivity are scant.

We have designed a modified premedication regimen, which includes a higher dose of dexamethasone (20 mg) plus an antihistamine. This dose of dexamethasone has been shown to be safe and effective for the prophylaxis of paclitaxel-associated hypersensitivity reactions [11]. Dexamethasone (20 mg) can be administered intravenously for desensitization against oxaliplatin hypersensitivity [3, 12]. These findings suggested that the prophylactic use of dexamethasone (20 mg) would reduce the incidence or severity of hypersensitivity reactions. We gave our modified regimen for premedication to patients with advanced colorectal cancer after they had received five cycles of a modified regimen of FOLFOX6 (mFOLFOX6) with standard premedication. We retrospectively compared the frequencies of hypersensitivity reactions between patients who received this modified premedication regimen with those who received standard premedication for the duration of FOLFOX treatment to determine whether our regimen was effective.

Patients and methods

Patient selection

This investigation was a retrospective cohort study of patients with advanced colorectal cancer who received modified FOLFOX6 (mFOLFOX6: oxaliplatin 85 mg/m^2 plus concurrent leucovorin 400 mg/m^2 as a 2-h intravenous infusion on day 1, followed by a bolus injection of 5-fluorouracil 400 mg/m^2 and by a 46-h continuous intravenous infusion of 5-fluorouracil 2,400 mg/m^2, repeated every 2 weeks) at Kinki University Hospital from September 2005 through September 2009. Eligible patients had to have adenocarcinoma of the colon or rectum; unresectable metastases; adequate bone marrow, liver, and kidney functions; a World Health Organization performance status of 0–2; and an age of ≥18 years. Patients who received five cycles of mFOLFOX6 without any allergic reactions were eligible. Patients with central nervous system metastases, only bone metastases, second malignancies, bowel obstruction, peripheral neuropathy of grade 3 or higher, symptomatic angina pectoris, or disease confined to previous radiation fields were excluded.

Chemotherapy and premedication

The patients were divided into two cohorts. In cohort 1, patients received routine premedication for the first five and subsequent cycles of mFOLFOX6 from September 2005 through September 2007. In cohort 2, treated between October 2007 and September 2009, patients similarly received routine premedication for the first five cycles. The premedication included routine antiemetic prophylaxis with dexamethasone 8 mg and granisetron 3 mg in 50 ml 0.9% saline, given intravenously 15 min before oxaliplatin. To reduce the risk of hypersensitivity reactions associated with continued treatment, from the sixth cycle onward all patients in cohort 2 received a modified premedication regimen, consisting of diphenhydramine 50 mg given orally 30 min before oxaliplatin, followed by dexamethasone 20 mg, granisetron 3 mg, and famotidine 20 mg in 50 ml saline, given intravenously 15 min before oxaliplatin.

Definition of allergic reactions

A hypersensitivity reaction to oxaliplatin was defined as the development of at least one of the following signs or symptoms after treatment with oxaliplatin: palmar erythema, pruritus, urticaria, diffuse erythroderma, tachycardia, angina, wheezing, facial or tongue edema, dyspnea, hypertension, hypotension, respiratory arrest, anaphylaxis, seizure, or death. Clinically significant respiratory compromise (wheezing associated with hypoxia or hypercarbia, and respiratory arrest), clinically significant cardiovascular compromise (angina, symptomatic hypotension or hypertension, and cardiovascular collapse), anaphylaxis, seizure, and death were all considered manifestations of a severe allergic reaction.

Study objectives and outcome measures

The primary objective of this study was to evaluate whether the modified premedication regimen reduced the incidence of hypersensitivity reactions. The primary outcome measure was the reduction in such reactions as compared with routine premedication. Secondary objectives were to evaluate the safety of the modified premedication regimen and to compare the duration of treatment with mFOLFOX6 and the reasons for treatment discontinuation between the two cohorts. Progressive disease was excluded from the analysis of reasons for treatment discontinuation.

Statistical analysis

A primary analysis was performed to compare cohorts 1 and 2. To assess the effect of premedication on hypersensitivity reactions to oxaliplatin in cohorts 1 and 2, we calculated risk ratios and 95% confidence intervals (95% CI). In addition, we calculated adjusted risk ratios with 95% CI for covariates (age, sex, diagnosis, prior treatment) by performing a Poisson regression analysis. To assess the effect of treatment exposure to the premedication on hypersensitivity reactions to oxaliplatin in cohorts 1 and 2, we compared the number of cycles between the cohorts with the use of the Wilcoxon test. All tests were two-sided with a significance level ≤ 0.05.

Results

Patient characteristics

The characteristics of the 181 eligible patients are listed in Table 1 (81 in cohort 1 and 100 in cohort 2). The patients' characteristics were well balanced between the cohorts, except for bevacizumab, because bevacizumab was approved in July 2007 in Japan. In 2007, bevacizumab was introduced to Japan; we therefore assessed the number of cycles administered for mFOLFOX6 alone in cohort 1 ($n = 81$) and for mFOLFOX6 alone ($n = 49$) and mFOLFOX6 plus bevacizumab ($n = 51$) in cohort 2. No patient in cohort 1 received bevacizumab, whereas nearly half the patients in cohort 2 received bevacizumab. No patient had a known history of allergy to a platinum salt. Five patients had a history of drug allergy.

Table 1 Patient characteristics

	Routine premedication (cohort 1)	Modified premedication (cohort 2)
No. of patients	81	100
Median age, years (range)	62 (29–82)	62 (34–84)
Sex		
Male/female	53/28	66/34
Diagnosis		
Colon	44	51
Rectum	37	49
Line of therapy		
First-line therapy	43	50
Second-line therapy	27	42
Third-line or subsequent therapy	11	8
mFOLFOX6 + bevacizumab	0	51
Median cumulative oxaliplatin dose for the first five cycles (mg/m^2)	414	419

FOLFOX6 chemotherapy with oxaliplatin plus fluorouracil and leucovorin

Incidence of hypersensitivity reactions to oxaliplatin

In cohort 1, hypersensitivity reactions developed in 16 (20%) of 81 patients who received routine premedication (Table 2). Six of these patients (7.4%) had manifestations of severe allergic reactions. In cohort 2, hypersensitivity reactions occurred in 7 (7.0%) of 100 patients who received modified premedication (Table 2). Three of these patients (3.0%) had manifestations of severe allergic reactions. The incidence of hypersensitivity reactions differed significantly between the cohorts (risk ratio, 0.3544; 95% CI, 0.1532–0.8196; $P = 0.0153$). Poisson regression analysis yielded a risk ratio of 0.3581 (95% CI, 0.1541–0.8324; $P = 0.0170$) (Table 2). None of the patients with a history of drug allergy had hypersensitivity reactions.

Treatment exposure

The 81 patients in cohort 1 received a total of 382 cycles of mFOLFOX6 (Table 2). The median number of cycles of mFOLFOX6 was 9 (9 as first-line therapy, 9 as second-line or subsequent therapy) (Table 3). The 100 patients in cohort 2 received a total of 781 cycles (Table 2). The median number of cycles of mFOLFOX6 was 12 overall (Table 2). The number of cycles differed significantly between the cohorts on the Wilcoxon test ($P < 0.0001$) (Table 2). In cohort 2, the median number of cycles of mFOLFOX6 without bevacizumab was 11 (10 as first-line therapy, 11 as second-line or subsequent therapy) (Table 3). The median number of cycles of mFOLFOX6 plus bevacizumab was 12 (12 as first-line therapy, 12 as second-line or subsequent therapy) (Table 3). The number of cycles in patients who additionally received bevacizumab did not differ significantly on the Wilcoxon test. The reasons for treatment

Table 2 Effect of premedication on incidence of hypersensitivity reactions to oxaliplatin

	Incidence of hypersensitivity reactions/ total patients (%)	Risk ratio (95% CI) (*P* value)	Adjusted risk ratio (95% CI) (*P* value)	Incidence of hypersensitivity reactions/total cycles (%)	Median cycles	*P* value
Routine premedication (cohort 1)	16/81 (20)	0.3544 (0.1532–0.8196) ($P = 0.0153$)	0.3581 (0.1541–0.8324) ($P = 0.0170$)	16/382 (4.2)	9	<0.0001
Modified premedication (cohort 2)	7/100 (7.0)			7/781 (0.90)	12	

CI confidence interval

Table 3 Effect of modified premedication on median number of treatment cycles

Cohort	Regimen	Line of therapy	Median cycles of mFOLFOX6 (range)	No. of patients
Routine premedication (cohort 1)	mFOLFOX6	First-line therapy	9 (6–17)	43
		Second-line or subsequent therapy	9 (6–22)	38
Modified premedication (cohort 2)	mFOLFOX6	First-line therapy	10 (6–28)	27
		Second-line or subsequent therapy	11 (6–29)	22
	mFOLFOX6 + bevacizumab	First-line therapy	12 (7–31)	23
		Second-line or subsequent therapy	12 (7–31)	28

discontinuation differed between the cohorts (Table 4). The main reason for treatment discontinuation in cohort 1 was hypersensitivity reactions (53%). Hypersensitivity was the second reason for discontinuing treatment in 11% of the patients in cohort 2. The main reason for treatment discontinuation in cohort 2 was neurotoxicity (53%). Neurotoxicity was the second reason for discontinuing treatment in 20% of the patients in cohort 1.

Table 4 Reasons for treatment discontinuation

Reasons for discontinuation	Routine premedication (cohort 1) ($n = 30$)		Modified premedication (cohort 2) ($n = 62$)	
	No. of patients	%	No. of patients	%
Neurotoxicity	6	20	33	53
Hypersensitivity reactions	16	53	7	11
Fatigue	0	0	3	4.8
Vomiting	0	0	2	3.2
Thrombocytopenia	0	0	1	1.6
Febrile neutropenia	2	6.7	4	6.5
Liver dysfunction	2	6.7	0	0
Thrombosis	0	0	1	1.6
Diarrhea	0	0	1	1.6
Others	4	13	10	16

Safety

Modified premedication did not increase the incidence of adverse effects related to the high dose of dexamethasone, such as exacerbation of diabetes, osteoporosis, and compression fracture. Diphenhydramine was associated with mild somnolence in two patients, but this symptom resolved promptly.

Discussion

The incidence of hypersensitivity reactions in cohort 1 was similar to that in previous studies. Allergic reactions usually develop after several infusions of oxaliplatin [13]. In cohort 2 of our study, the use of modified premedication decreased the incidence of hypersensitivity reactions to 7.0%. Modified premedication with increased doses of dexamethasone and antihistamines thus reduced the incidence of hypersensitivity reactions by 14 percentage points as compared with cohort 1, treated with routine premedication. Gowda et al. [9] evaluated the incidence of hypersensitivity reactions to oxaliplatin and reported 32 hypersensitivity reactions in 169 patients (incidence, 18.9%) who received oxaliplatin preceded by dexamethasone (10 mg) and ondansetron (Zofran, 8 mg). Brandi et al. [7] reported that hypersensitivity reactions occurred in 18.1% of patients who received oxaliplatin preceded by ondansetron. Other than these reports, studies assessing the